

UC Davis

UC Davis Previously Published Works

Title

Biomedical applications of electrical stimulation

Permalink

<https://escholarship.org/uc/item/7z16276q>

Journal

Cellular and Molecular Life Sciences, 77(14)

ISSN

1420-682X

Authors

Zhao, Siwei

Mehta, Abijeet Singh

Zhao, Min

Publication Date

2020-07-01

DOI

10.1007/s00018-019-03446-1

Peer reviewed



Published in final edited form as:

Cell Mol Life Sci. 2020 July ; 77(14): 2681–2699. doi:10.1007/s00018-019-03446-1.

Biomedical Applications of Electrical Stimulation

Siwei Zhao^{1,2,*}, Abijeet Mehta³, Min Zhao³

¹Mary and Dick Holland Regenerative Medicine Program, University of Nebraska Medical Center, 985965 Nebraska Medical Center, Omaha, NE 68198, USA

²Department of Surgery, University of Nebraska Medical Center, 985965 Nebraska Medical Center, Omaha, NE 68198, USA

³Department of Dermatology, University of California, Davis, CA, USA

Abstract

This review provides a comprehensive overview on the biomedical applications of electrical stimulation (EStim). EStim has a wide range of direct effects on both biomolecules and cells. These effects have been exploited to facilitate proliferation and functional development of engineered tissue constructs for regenerative medicine applications. They have also been tested or used in clinics for pain mitigation, muscle rehabilitation, the treatment of motor/consciousness disorders, wound healing, and drug delivery. However, the research on fundamental mechanism of cellular response to EStim has fell behind its applications, which has hindered the full exploitation of the clinical potential of EStim. Moreover, despite the positive outcome from the in vitro and animal studies testing efficacy of EStim, existing clinical trials failed to establish strong, conclusive supports for the therapeutic efficacy of EStim for most of the clinical applications mentioned above. Two potential directions of future research to improve clinical utility of EStim are presented, including the optimization and standardization of stimulation protocol and the development of more tissue-matching devices.

Keywords

Electrical Stimulation; Tissue Engineering; Clinical Trial; Ocular Drug Delivery; Iontophoresis; Wound Healing

1. Introduction

EStim is a non-invasive and non-pharmacological physical stimulus. EStim has a broad range of biomedical effects (Figure 1). At the molecular level, it can facilitate the transport of both charged and uncharged biomolecules through biological membranes via electrophoresis and electroosmosis. These two processes collectively are called iontophoresis (1). At the cellular level, EStim can interact with a variety of cellular

*Correspondence: Siwei Zhao. siwei.zhao@unmc.edu; Tel.: +1-402-559-9952.

Author Contributions: S. Zhao and M. Zhao conceived the idea for the article. All authors performed the literature search. All authors drafted and critically revised the work. All authors have read and approved the submitted version of the manuscript.

Conflicts of Interest: The authors declare no conflict of interest.

components, such as ion channels, membrane-bound proteins, cytoskeleton and intracellular organelles (2). These interactions alter cellular activities and functions, such as contraction, migration, orientation and proliferation (3, 4).

Due to these direct effects on biomolecules and cells, EStim has been utilized in a wide range of biomedical and clinical applications. EStim is frequently utilized in tissue engineering and regenerative medicine to provide electrical cues to facilitate cell proliferation, stem cell differentiation, tissue regeneration, as well as remodeling and maturation of engineered tissue constructs (2). For example, EStim has been widely used in neural tissue engineering. The effects of EStim include the accelerated and directional neurite and axon growth, and the differentiation of embryonic stem cell into the neural fate (5). Many different types of EStim have been tested and demonstrated efficacy for neural tissue engineering, including direct current (DC), alternating current (AC), pulsed current (PC) and pulsed electromagnetic fields (PEMF). EStim has shown efficacy in muscle tissue engineering. In skeletal muscle tissue engineering, EStim has shown to be able to promote the proliferation of myoblasts, the fusion of myoblasts to myotubes, and the expression of myosin heavy chain (6-8). In cardiac tissue engineering, EStim has been frequently used to facilitate the functional maturation of stem cell-derived or fetal cardiomyocytes (CMs), including the alignment and elongation of CMs, the increased expression of connexin 43 and troponin-I, as well as the synchronous contractions of CMs within constructs (9). PC EStim is usually used for the stimulation of muscle tissue constructs. EStim has been used to stimulate bone regeneration (10-12). In vitro studies have shown that EStim can stimulate calcium signaling and increase bone formation (11). EStim can also upregulate the production of bone growth factors (11). When DC EStim is used, the cathode electrochemical reactions generate hydroxide ions and hydrogen peroxide, which have shown to stimulate osteoblast and VEGF production by macrophages (11). DC, AC, PC and PEMF EStim modes have been tested and shown efficacy for bone tissue regeneration. EStim has also shown to facilitate wound healing (13-15). EStim contributes to healing wounds by enhancing the proliferation of skin cells, inducing directional migration of skin cells, providing the bacteriostatic and bactericidal effects, and increasing blood perfusion (13). DC, AC, PC and PEMF have all been utilized in wound healing.

Besides the regenerative medicine, EStim has also been proposed as an alternative treatment modality to conventional pharmacological interventions and an effective drug delivery method for a variety of diseases. The utility of EStim on pain management has been extensively studied. Some evidence has shown that EStim has the potential to reduce neck pain (16), post-operative pain (17), cancer pain (18), chronic pain (19, 20), diabetic peripheral neuropathy (21), and osteoarthritic knee pain (22, 23). Moreover, it has been reported that EStim is capable of improving muscle contraction force and maintaining muscle mass and strength after nerve injuries, which is particularly useful in sports medicine and rehabilitation after injury (24). Transcranial direct current stimulation (tDCS) has been used to treat Parkinson's disease (25), aphasia (26), multiple sclerosis (27), epilepsy (28), Alzheimer's disease (29), tinnitus (30), depression (31), addiction and craving (32). It has received level B recommendation (i.e. probable efficacy) for fibromyalgia, depression and craving/addiction in a recent literature survey on the state-of-the-art of the therapeutic use of tDCS (33). In addition, a large number of studies have shown that iontophoresis can

significantly increase the drug delivery efficiency through tissue barriers, such as skin and cornea compared to passive diffusion (34-36). As aforementioned, iontophoresis consists of two physical processes, the electrophoresis and the electroosmosis (Figure 1, left panel) (1). Electrophoresis alters the mobility of charged drug molecules through the Coulomb force the electrical field exerts on those molecules. Electroosmosis induces a solvent flow across an ionized membranes due to the electrical force exerted on the thin electric double layers. The direction of the flow depends on the charge of the biological membrane. For skin and cornea, the flow is from anode to cathode. The drug molecules in the solvent flow in the same direction due to fluid drag force. Therefore, neutral drug molecules can be transported by electroosmosis. Electrophoresis and electroosmosis always happen simultaneously, their relative strength determines the net flow direction of the drug molecules.

The EStim conditions commonly used for each type of application and the typical effects of EStim are summarized in Table 1.

The hardware for EStim application has been revolutionized over the last several decades due to the development of novel materials and new device architectures. Macroscale rod- or wire-shaped electrodes are conventionally inserted in tissue culture medium to delivery EStim (40). However, microfabricated electrodes have started to gain popularity due to their capability to integrate in engineered scaffolds to provide localized and directional EStim (41, 42). For therapeutic EStim, electrodes pads are often placed on the skin at the target location to deliver EStim. More recently, the advancement in material science and circuit design has enabled the development of electrical circuit on soft and stretchable substrates that have programmable life time. This has led to wearable and degradable EStim devices that allow more convenient and continuous EStim therapy (43, 44).

In this review, our objective is to: 1) discuss the fundamental mechanisms of tissue and cellular response to EStim; 2) review in vitro high-throughput and tissue engineering devices that are developed to either study or utilize EStim; 3) review clinical evidence on the efficacy of EStim for wound healing and ocular drug delivery; and 4) discuss the critical needs and gaps for the future development of therapeutic EStim. The term “electrical stimulation” in our review has a broad meaning. It refers to not only the physiological stimulation of cellular and tissue activities through the application of electrical field or current, but also the physical “stimulation” of faster molecular transports through biological membranes.

2. Mechanisms of Cellular Response to Estim

Common cellular responses to EStim include adhesion, proliferation, differentiation, directional migration, and cell division. For nerve cells, it has been reported that EStim enhances oligodendrocyte maturation and myelin formation (45), neural precursor migration in mouse brains in vivo (46), promotes nerve cell regeneration and stimulates Schwann cells to express neurotrophic factors (47). EStim of injured peripheral nerves has accelerated axonal regeneration in laboratory animals (48, 49). For bone cells, EStim of osteoblasts promotes natural healing of fracture bone break cases in humans (50), enhances osteoblast cells activity (51). AC EStim has shown to promote bone regeneration by promoting

differentiation of osteoblastic cells (52), and the osteogenic differentiation of human mesenchymal stem cells (hMSCs) (53). For muscle cells, nanosecond pulsed electric field can modulate myoblast for proliferation and differentiation (54). EStim of the skeletal muscle bundles can be used to study contraction-dependent endocrine effects of myokines on the activity of co-cultured monocytes (55). Exposure of mouse myoblast cells to an electrical field resulted in morphological alterations with elongated nucleus, roughening of the cell surface topography, and myogenesis (56). For skin cells, EStim has shown to guide the migration of epidermal stem cells (EpSCs) to regulate wound healing (57). EStim can shift injury response from healing/scarring towards regeneration by promoting cell proliferation, generating less condensed collagen fibrils, and by modifying macrophage responses (58). AC EStim of 50 μ A, generated by a triboelectric nanogenerator (TENG), have shown to promote fibroblast cell proliferation (59).

The fundamental physical mechanisms that are responsible for the aforementioned cellular responses to EStim are currently under active research. A number of hypotheses have been proposed, which are summarized here. 1) Structural water disruption: EStim can lead to immediate disruption in the ordered arrangement of dipolar water (i.e. structured water) surrounding both the external surface of cell as well as the cell cortex (60, 61). This effect causes cell to loss its gel structure to become more of a sol, and releases large amount of trapped calcium ions leading to a calcium wave. Disruption of extracellular structured water also allows rapid influx of Na^+ ions with an opposite flow of K^+ outside the cell. This transition leads to the lamellipodial protrusion at the leading edge of the cell and its concomitant directional mobility. The ion flux can also affect cell volume and membrane potential (62). 2) Electroosmotic fluid flow: in addition to accelerating trans-membrane drug delivery, the electroosmosis induced by the application of an electrical field can also generate forces acting on the surface of the cell. These forces reorient the cell through a form of hydrodynamic drag force (F_{HD}) (63). This effect occurs because of the partitioning of larger Na^+ ions externally, and small K^+ ions internally across the cell membrane. Larger Na^+ ions attract larger aqueous shell of water molecule externally as compared to small shell of water molecules attracted by K^+ ions internally. This difference can create strong external dragging force in the presence of electrical field resulting in cell mobility (64), and intracellular transport of biomolecules (65). The electroosmotic forces can have various phenotypic effects including cell proliferation, cell differentiation, and embryogenesis (66, 67). 3) Asymmetric ion flow and opening of voltage gated channels: the application of electrical field to cell will asymmetrically hyperpolarize the anodal side, and depolarize the cathodal side of the cell thus modulating the cell membrane potential resulting into change in activity of voltage gated sodium, potassium, and calcium channels. This change creates asymmetric electromotive force for ions to flow once ion-channels are open (68). This electromotive force is also called electrostatic force (F_e) (69). Similarly, In the presence of electrical field, intracellular polyamines accumulate toward the cathode side, increasing inward rectifying property of KCNJ15/Kir4.2, and blocking influx of K^+ ions (70). However, the anode side will show decreased inward rectifying property. This biased inward rectifying property of potassium channels to the cathode side will result in asymmetric flow of K^+ ions. This asymmetric ion flow and opening of voltage gated ion channels can lead to various cellular responses effecting the final phenotype. For example, K^+ waves integrate

Pseudomonas aeruginosa cells and *Bacillus subtilis* cell in the biofilm soma (71); ion channel signaling affects limb and spinal cord regeneration in vertebrates (72, 73); active inwardly rectifying potassium (Irk) channels regulate release of the *Drosophila* bone morphogenetic protein Dpp, which is necessary for normal wing morphogenesis (74); electric synapses modulate eye size and border cell fate via DPP signaling in *Drosophila* (75, 76); ion-channel-dependent signaling causing developmental defects in mammals (77). 4) Mechanosensation: the electrostatic and electroosmotic forces induced by the electrical field will apply mechanical forces (F_m) on the tension sensitive components on cell surface, e.g. focal adhesion and cadherin adhesion. As a result, cell components will be dragged laterally. These mechanical signals alter the downstream gene expression and signaling pathways (i.e. mechanotransduction), causing change in various cellular processes, including cell mobility, cell proliferation, organogenesis, and development (78-80). For example, mechanosensitive pathways such as Notch, Wnt/Ang2, play crucial roles in cardiovascular development and homeostasis in zebrafish model (81). 5) Redistribution of membrane components and lipid rafts: F_e , F_{HD} , at the plasma membrane will create cathodal-anodal axis of polarity by redistributing charged particles of the membrane (82). Similarly, the three forces (F_e , F_{HD} , and F_m) generated by applied electrical field can induce forces on the lipid rafts resulting in its asymmetric redistribution across the cell membrane (83). This preferential distribution further polarizes cell membrane components e.g. integrin, and caveolin, which in positive feedback loop with lipid raft redistribution promotes raft structural stabilization. This polarized effect of electrical field can lead to directional mobility of cells. Previous reports on the effect of integrin type on the direction of cell migration (84) makes feed-forward interaction between lipid rafts and integrin effect on cell mobility even more interesting. This redistribution of membrane components and lipid rafts can bring changes in cell-to-cell communication and the initiation of intracellular signals among other pathophysiological functions (85). The above mentioned hypotheses have been summarized in Figure 2.

All of these putative sensors of external electrical field relay information through receptor-based cell signaling to different partners of intracellular components who act as a microprocessor that processes the electrical code, gets perturbed and transforms the electrical signal into cellular responses. Here we use cell mobility as an example to illustrate some of the downstream signaling pathways that may be involved to elicit cellular responses (86, 87). The electrical field-induced passive accumulation of Ca^{2+} ions at the anodal side of the cell is sufficient to induce contraction of the cytoskeleton and propel the cell towards the cathode (88). However, cytoskeleton perturbation does not provide sufficient evidence to explain the molecular mechanism of electrical field-induced cellular response. Clearly, some intracellular signaling pathways may also play roles in how cell behavior is altered in the presence of external electrical field. PI3K-AKT (phosphoinositide-3 kinase-AKT serine/threonine kinase) and PTEN (phosphatase and tensin homolog) gene are the two key molecules that were discovered playing crucial role in electrical field-induced cell migration (89). Genetic disruption of PI3 kinase γ abolishes directed cell movement, and deletion of the PTEN (an antagonist of the PI3K-AKT pathway), upregulates PI3K-AKT signaling axis, that enhances the electrical field-induced cellular responses. Similarly, effect of DC electrical field, on both keratinocytes and corneal epithelial involving epidermal growth factor receptor (EGFR) has also been reported (90, 91). This concept is further corroborated

by asymmetric distribution of increased lamellipodial Ca^{2+} sparks, relocation of extracellular signal-regulated kinase 1, 2 (ERK1, 2), pERK1, 2 (phosphorated ERK1, 2), and asymmetric activation of EGFR by Estim (92-94).

3. In Vitro Systems That Study or Utilize EStim

3.1. High-Throughput Platforms for Studying Cellular Response to EStim

To fully exploit the therapeutic potential of EStim, it is necessary to elucidate the fundamental mechanisms of cellular responses to EStim and to identify the most effective and safe EStim conditions for different application scenarios. Conventional experimental setups for studying cellular response to EStim, such as the electrotaxis chamber, have limited throughput. They usually can only test one condition or one type of cell in each experiment. This low throughput has significantly hindered the progress of EStim-related discoveries for both fundamental research and clinical applications.

To address this issue, high-throughput and integrated testing systems have been developed that are capable of testing multiple EStim conditions or cell types in one experiment. The most commonly used high-throughput experimental setup is the multiwell plate. In two studies from Barker's group (95, 96), a 6-well plate-based high-throughput experimental setup was developed to investigate the effects of different EStim parameters, including electrical field strength and EStim duration on the osteogenic differentiation of mesenchymal stem cells (MSCs). The L-shaped EStim electrodes were attached to the lid of the 6-well plate, and were able to deliver uniform EStim to each individual well. In another study by Du et al. (97), a 96-well plate-based high-throughput screening platform was developed for studying the optimal EStim parameters for human neural crest stem cell (NCSC) differentiation. The EStim electrodes were arranged in a top-down configuration to generate a vertical electrical field that can stimulate a larger area. The parameters investigated include EStim frequency, duration and the direction of electrical field.

More recently, microfabricated platforms, such as microfluidics and lab-on-a-chips, have been used in EStim studies, which have significantly improved the throughput. Microfluidics channels with changing widths (98, 99) (Figure 3A) or resistor-ladder design (100, 101) (Figure 3B) have been developed to generate multiple EStim strengths, which can be studied in the same device in one experiment. Among these devices, the resistor-ladder design is capable of generating a wide range of EStim intensity spanning over three orders of magnitude from 2.1 mV/mm to 1.6 V/mm using a simple and expandable channel layout (100). Salt bridges, power supply and/or voltage meter have been integrated in these systems, minimizing the footprint of the experimental setup. System that allows multiple different cells to be tested in the same experiment was also developed. Gao and colleagues developed a barcoded microplate-based platform to study the EStim response of a library of 563 *Dictyostelium discoideum* strains with morphological defects (102) (Figure 3C). Each microplate had a unique graphic barcode which was correlated with the *Dictyostelium discoideum* strain that it carried. Up to 30 types of microplates/strains were loaded in a testing chamber and their response to EStim was studied in one experiment. This study identified a number of genes that mediate the electrotaxis of *Dictyostelium discoideum*. These studies have significant impact in the field. They collectively provide the

technological advancement that is necessary to elucidate the molecular mechanisms of electrotaxis and to identify the effective and safe stimulation conditions for clinical utilities.

The optimal EStim parameters found in high-throughput studies have benefited tissue engineering applications. A study from Vunjak-Novakovic's group (103) used a miniaturized experimental platform and high-throughput method to identify the optimal electrode material and electrical parameters, including amplitude and frequency, for the EStim of neonatal rat cardiomyocytes. The optimal EStim condition they identified have been used in many cardiac tissue engineering studies to improve cell morphology, the production of proteins that are specific to cardiac gap junctions and contraction, and the contraction force (104, 105). The best EStim conditions found in Barker's studies (95, 96) have been used in a recently published study (12) to enhance the osteogenic differentiation of bone tissue engineering constructs with encapsulated MSCs. In the same study, the optimal EStim condition was also applied to bone tissue engineering constructs that were implanted to treat rat femur large defects. The EStim therapy significantly improved the healing of rat femur large defects, with higher bone formation, strength and increased expression of osteogenic genes. The optimal EStim parameters identified in the study by Du et al. (97) was applied to NCSCs that were transplanted in live animals with sciatic nerve injuries. It was found this EStim protocol significantly enhanced the survival rate and differentiation of the transplanted NCSCs, as well as the overall nerve regeneration. These results show that high-throughput EStim studies have provided practical guidance on the selection of optimal EStim conditions for tissue engineering applications.

3.2. Tissue Engineering Systems that Utilize EStim

Due to its direct effects on cells and the crucial role of electrical signal in early tissue development and regeneration, EStim has been widely integrated in tissue engineering systems or applied during in vivo tissue regeneration to improve tissue proliferation, remodeling and maturation (2). It has been shown that EStim applied directly to tissue scaffolds could significantly enhance the nerve cell proliferation and neurite outgrowth in vitro (106-109) (Figure 4A), as well as axonal regeneration/remyelination and functional recovery in vivo (110-112) compared to the same scaffolds without EStim. EStim has also been applied to engineered skeletal muscle tissues. It was reported that the application of EStim improved the myobundle size, muscle contraction force and the expression of genes related to sarcomere development (113-115) (Figure 4B). Due to the importance of electrical cues and activities in the development and functions of cardiac tissue, EStim has been widely used in cardiac tissue engineering. It has been shown that EStim could improve the assembly and the functional development of neonatal rat cardiomyocytes into cardiac tissues that exhibited contractile capability (103, 104, 116) (Figure 4C). EStim has also been applied to bone tissue engineering constructs to enhance the differentiation of stem cells into osteo-lineage and the functional maturation of the tissues. For example, in two studies by Hu et al., a biocompatible polypyrrole scaffold with adjustable electrical conductivity was developed (117, 118). Rat bone marrow stromal cells (rBMSCs) were seeded on the scaffolds and electrically stimulated. It was found that the conductive scaffolds and the EStim significantly accelerated the differentiation of rBMSCs and enhanced their

mineralization. A detailed evaluation of different EStim modes revealed that square wave at 200mV/mm electrical field strength delivered the best outcomes.

EStim can be directly applied to the tissue culture medium as in the case of cardiac tissue EStim (40) (Figure 5A). Electrodes are typically made of inert materials, such as carbon and platinum (42, 119). It is also a common practice to apply EStim through conductive scaffolds, which are typically made of conducting polymer fibers or carbon nanomaterials (5, 120, 121) (Figure 5B). These conductive scaffolds have attracted much attention recently, because they are not only capable of delivering localized EStim to the cells that are attached to the scaffolds (106, 107, 122), but also able to provide topographic cues for cell orientation and proliferation (123, 124). Conducting polymers and carbon nanomaterials are easy to be modified to allow better tissue interfaces and functions. Extracellular components (e.g. laminin fragments and RGD motifs) and bioactive molecules (e.g. hyaluronic acid) have been blended in or grafted to the surface of the conducting polymer fibers (125-127). Functional groups (e.g. carboxyl group) and biomolecules (e.g. polyethyleneimine and phospholipids) have been grafted on the surface of carbon nanotubes to improve their biocompatibility and functions (128).

4. The Clinical Utilities of EStim

As aforementioned, EStim has many potential clinical applications as a non-invasive and non-pharmacological therapeutic modality. However, for many of the applications that have been tested, there is a lack of strong clinical evidence that supports the therapeutic efficacy of EStim. For example, two recent reviews summarized the clinical evidence for the use of EStim in bone regeneration in human patients (11, 129). They found the existing clinical trials have reported inconclusive and mixed results regarding the clinical efficacy of EStim on bone repair. The evidence provided by many clinical trials was of limited quality due to the small sample size, poorly designed controls and/or variability in fracture sites. The efficacy of EStim on the restoration and recovery of denervated muscles is also inconsistent (130). According to the literature, the EStim efficacy is highly dependent on the EStim conditions: higher current intensities and longer pulse widths usually generated better outcomes, especially in human muscles that have been denervated for long time (38, 131). However, such high current intensities and long pulse widths can cause serious tissue damage (132-134), so it is unclear how useful they are in a clinical setup. Very few clinical trials have tested the efficacy of EStim on nerve regeneration in human subjects. One randomized controlled clinical trial compared the effects EStim on sensory nerve regeneration with no-EStim control (135). Although a trend of greater functional improvements was shown in the EStim group when compared to the control, the difference was not statistically significant. Another randomized controlled clinical trial aimed to determine the efficacy of EStim on axonal regeneration after surgery (136, 137). The EStim group showed faster motor neuron regeneration than the control group. However, the EStim group failed to show significantly greater improvement in motor performance when compared to the control. Transcutaneous electrical nerve stimulation (TENS) has been frequently used for pain relief. A recently published systemic review surveyed the efficacy of TENS in pain reduction in human patients (138). It concluded that the existing studies showed conflicting outcomes: some showed efficacy while the others showed no

improvement. Another problem is the lack of high-quality clinical studies and the inconsistency in TENS parameters used in the existing studies.

There are two EStim application areas that have been extensively studied in animal models and clinical trials and have generated relatively consistent positive outcomes, which are the EStim-assisted wound healing and the iontophoretic drug delivery. For iontophoretic drug delivery, we are particularly interested in ocular drug delivery, because EStim is non-invasive and enables high drug delivery efficiency, two attributes highly desired for ocular applications that are not offered by any of the conventional methods. Therefore, we will focus our discussion in this section on EStim-assisted wound healing and iontophoretic ocular drug delivery.

4.1. Electrical Field Assisted Wound Healing

As aforementioned, the application of external EStim can enhance the migration directedness and/or speed of a variety of cell types, including cells that actively participate in the wound healing process, such as keratinocytes (139, 140) and dermal fibroblasts (141, 142). EStim has been successfully used to speed up the healing of in vitro scratch wounds, indicating strong therapeutic potentials.

A number of clinical trials have been conducted in the last 3 decades to assess the efficacy of EStim on enhancing the healing of various chronic wounds (143-152). Pulsed direct current is the most commonly used form of EStim. DC electrical field provides the directional cue that is necessary to guide cell migration into the wound bed. The pulsed signal reduces the time when the voltage is on so that the adverse effects, such as local heating and chemical changes, do not accumulate on tissue surface. Continuous DC EStim is also used. However, the intensity has to be kept low to avoid tissue damage.

Many studies have reported that the application of EStim was able to significantly enhance the wound healing speed and/or the number of wounds closed at the end of the study, compared to conventional wound care. For example, using a pulsed DC EStim at a low current intensity of 600 μ A, Wood and colleagues reported that EStim significantly increased the number of wounds healed at the end of the study compared to sham control ($P < 0.0001$) (144). Lundeborg and colleagues reported that the application of pulsed EStim signal could significantly increase both the number of wounds healed and the wound healing speed ($P < 0.05$) (149). Carley and colleagues have shown that continuous, low-intensity DC EStim could effectively increase wound closing speed compared to the control ($P < 0.01$) (150). Houghton (147) and Lawson (152) in two separate reports demonstrated that pulsed EStim with high-intensity could effectively increase wound healing speed ($P < 0.05$ and $P < 0.01$, respectively).

Other studies have reported less encouraging findings on the effect of EStim on wound healing, which were either insignificant improvement compared to control or no improvement. For example, Peters (143), Adunsky (148), Griffin (146) and Houghton (145) in their respective reports have shown that high-voltage, pulsed DC EStim could enhance the wound healing speed and/or the number of wounds healed compared to control, but the differences were not significant ($P > 0.05$). In the study conducted by Feedar and colleagues

(153), it was found that high-voltage, pulsed DC EStim could effectively improve the wound healing speed compared the sham control ($P < 0.02$), but the number of wounds healed at the end of the four-week study was fewer than sham control, although not significant ($P > 0.05$).

Commercial wound dressings with EStim capabilities are being developed. POSiFECT® is one of the early products developed by Biofisica, Inc. (154) (Figure 6A). It is a disposable wound dressing device capable of delivering EStim to facilitate the wound healing process. The POSiFECT device represents a typical design of EStim wound dressing, consisting of a ring-shaped anode placed on the outside of the wound and a small cathode placed at the center of the wound bed to direct the electrical field/current toward the wound bed. The power is provided by an integrated battery module and a constant EStim current is ensured through a control circuit. Procellera® is a wound dressing device currently under active development by Vomaris Innovations, Inc. (155) (Figure 6B). It integrates a novel micro-cell battery array that the company claims uses in situ electrochemical reactions to generate EStim current for wound stimulation. It has been shown that Procellera wound dressing had antibacterial effects against clinical wound pathogens, which could reduce the risk of infection at wound site and thus facilitate the wound healing process (156). A controlled, preclinical study has been conducted that provided in vivo evidence on the anti-biofilm efficacy of Procellera wound dressing. WoundEL® is a commercial EStim device that can deliver low voltage, pulsed current to facilitate the wound heal process and reduce wound related pain. A human clinical trial demonstrated that the WoundEL treatment of leg ulcers for 3 and 7 days could significantly reduce the pain score compared to the onset of the study (157). The use of analgesic treatments could thus be reduced. A Dacron-mesh silver nylon stocking has been used as a wearable electrode to deliver EStim wound treatment during night time. Compared to conventional electrodes, these stocking electrodes provided long-term EStim capability along with comfort (143).

4.2. Iontophoretic Ocular Drug Delivery

Another area of clinical utility of EStim that has attracted much attention is the iontophoretic ocular drug delivery. Iontophoresis, as aforementioned, can significantly increase the trans-membrane transport of biomolecules without affecting tissues given that the EStim energy is within a safe range. Due to its non-invasiveness and high drug transport efficiency, iontophoresis has been tested for drug delivery into the eye, which is an organ where conventional drug delivery routes (e.g. systemic and topical delivery) have low efficiency. DC EStim is the primary approach used in this type of application, because a constant electrical field direction is required to continuously “push” drug molecules into the eye tissue. The iontophoretic ocular drug delivery typically uses two routes, the trans-corneal route and the trans-scleral route. For trans-corneal iontophoresis, the working electrode and the drug reservoir are typically placed on the cornea. Drug molecules would penetrate cornea under the guidance of electrical field and eventually get delivered into the anterior segment. This route is used to treat anterior segment diseases, such as glaucoma, dry eyes and keratitis. For trans-scleral iontophoresis, working electrodes are usually placed at the pars plana on the sclera. Drug molecules would penetrate sclera and choroid and eventually get delivered into the retina or the vitreous. This route is used to treat posterior segment diseases, such as age-related macular degeneration. For both routes, the counter electrode is

typically placed on the ear (158, 159). A recent study showed that effective ocular iontophoresis could also be achieved when both working and counter electrodes were placed on the same eye (160).

Trans-corneal iontophoresis has been frequently used to deliver riboflavin, which is a chemical used in combination with ultraviolet (UV) irradiation to crosslink and stiffen cornea (161). In a clinical trial published in 2014, trans-corneal iontophoresis was performed in 19 patients (22 eyes) to deliver riboflavin into the cornea, which was subsequently used to crosslink the cornea by UV irradiation to treat progressive keratoconus (162). It was found that the riboflavin/UVA treatment resulted in decreases in both keratometry level and corneal astigmatism, and improved the uncorrected distance visual acuity from 0.61 ± 0.44 up to 0.48 ± 0.41 (LogMAR) one year after the procedure. A more recent randomized controlled clinical trial compared the outcomes of the trans-epithelial iontophoresis-assisted corneal crosslinking and the standard corneal crosslinking with the epithelial layer removed (epi-off) (163). At 6-month post procedure, the iontophoresis group resulted in a significantly higher corrected distance visual acuity compared to the standard epi-off corneal crosslinking. However, at 24-month, the difference was not significant any more. Also after 24 months, the iontophoresis was less effective than the standard corneal crosslinking on the stabilization and regression of keratometry values. It was found that iontophoresis had a less penetration depth of riboflavin than the standard method with epi-off.

Trans-scleral iontophoresis has been used to deliver corticosteroids to the posterior segment. Two separate clinical trials studied the effectiveness of a trans-scleral iontophoresis device, EyeGate II, on delivering EGP-437 (a dexamethasone phosphate formulated for iontophoresis) for treating dry eye (164) and noninfectious anterior uveitis (165). The first study showed that the iontophoretic delivery of EGP-437 significantly improved the signs and symptoms of dry eye, including corneal staining, ocular protection index and ocular discomfort, compared to placebo control where sodium citrate buffer solution was used instead of dexamethasone. The second study tested a range of different EStim intensity (1.6, 4.8, 10.0, or 14.0 mA-min) for the delivery of EGP-437 and assessed their efficacy in treating noninfectious anterior uveitis. It was found that the lower doses seemed to be the most effective, and all treatments were well-tolerated. The same EyeGate II device has also been used to deliver another corticosteroid, methylprednisolone sodium succinate, into the cornea through trans-scleral iontophoresis followed by lateral diffusion (166). It was shown that this method was effective in reducing active corneal graft rejection and improving corrected visual acuity.

Commercial iontophoretic devices have been developed to target ocular drug delivery. As aforementioned, EyeGate II, developed by EyeGate Pharma, uses trans-scleral iontophoresis to deliver therapeutic concentration of drug molecules into various ocular tissues (165) (Figure 7A). The most commonly delivered drug is EGP-437, which is a dexamethasone phosphate optimized specifically for iontophoresis. Last year, the company announced on their website the outcomes of its Phase 3 clinical study on the safety and efficacy of EGP-437 delivered by the EyeGate II device. Although the iontophoretically delivered EGP-437 showed therapeutic efficacy, it was inferior to the positive control which used the standard prednisolone acetate. OcuPhor was another ocular iontophoretic device that was

once under investigation (167) (Figure 7B). It had a simpler design compared to the EyeGate II system, and used the same trans-scleral route. Human clinical study was conducted to evaluate the safety of Ocuphor device in healthy volunteers and found that it was in general safe if the dose is less than 3 mA for 20 min or 1.5 mA for 40 min (168). However, no new studies on Ocuphor can be found after 2003.

5. Problems and Perspectives

5.1. The Need to Unveil the Fundamental Mechanism of Cellular Response to EStim

To apply EStim-based therapies to cure diseases, and improve biological processes like tissue regeneration there is a dire need to unveil mechanism of how exactly cell behaves in the electrical field. The mechanisms behind cell–EStim interactions are not yet well understood. The difficulty to understand mechanisms for EStim–cell interaction calls for a detailed understanding of the induced EStim structures in cells. This first requires thorough knowledge about ion channel targets expressed in tissues of interest so that they can then be accordingly manipulated using EStim. Recently a bioinformatics platform, electroceutical design environment (EDEn), has been designed that includes information on ion channels and ion pumps, linked to known chemical modulators and their properties (169). The database also provides information about the expression levels of the ion channels in over 100 tissue types. This database can help us to determine which ion channels should be manipulated by electroceuticals or EStim to bring downstream changes in transcriptional and epigenetic profile resulting in modifying current state (diseased or immature) to desired state. Also construction of mathematical models is especially crucial to improve understanding of these ion-channel, and how cells behave in external electrical field. Various such mathematical models have been proposed before. For example, Fricke and Schwan model predicted the potential induced in an ellipsoidal and spherical cell respectively within the suspension exposed to external EStim (170, 171). Numeric finite-element modelling (FEM) (172), transport lattice (TLM) models (173), and approaches based on equivalent circuits (174) examined complex cells of complex shapes immersed in an electrolyte. However in many in vivo conditions cells behavior towards EStim is more dynamic involving complex feedback loops therefore next road map in this effort is to develop machine learning based computation platforms e.g. BioElectric Tissue Simulation Engine (BETSE), a finite volume method multiphysics simulator that can predict the origin and progression of local and long-range bioelectric patterns in complex multicellular tissues (175). In future such efforts, along with their clinical trials can open new windows in the field of bioelectricity-based therapies.

5.2. The Need to Standardize and Improve Therapeutic Estim Protocol and Device

Although EStim has a broad range of therapeutic potentials, it has not been widely accepted in everyday clinical practice. This is because its therapeutic efficacy is inconsistent and inconclusive. After careful review of the published clinical studies, we think there are three reasons that are potentially responsible for such inconsistent outcomes.

First, a variety of different EStim conditions have been used the clinical studies, including different voltages, currents, duration, waveform and polarity. Some studies were voltage-

controlled, some were current-controlled. These diverse experimental conditions make it very difficult to compare results from different clinical studies or to reach any reliable conclusion. It is also impossible to establish any guidance for future implementation of EStim in the clinics. There is a critical need for systemic studies to identify optimal EStim conditions for each application. The fundamental mechanism of EStim response of different cell/tissue types would help to unveil such information.

Second, most of the published studies did not monitor how much EStim was actually delivered to the target tissues. EStim energy may be lost in the circuit or at the circuit/tissue interface. The heterogeneous tissue structures and electrical properties could lead to a highly non-uniform electrical field distribution. All these factors would affect the amplitude of the EStim signal that is delivered to the target tissues. In addition, dynamic effects should also be considered, such as the change of the impedance at circuit/tissue interface during EStim application (176). It is necessary to establish a detailed electrical model for each different tissue type to help predict the spatial and dynamic distribution of the EStim signal. It is also necessary to perform real-time EStim monitoring at the target tissue during EStim application to ensure the desired EStim intensity is delivered and the outcome is reproducible.

Third, the EStim delivery capacity of current electrical devices is largely limited. There are fundamental differences between current electrical systems and biological tissues, including the type of current conducted and their mechanical properties. All current electrical circuits conduct electron currents. Biological tissues, however, use ion currents. In order to deliver EStim to tissues, the electron currents have to be converted to ion currents through electrochemical reactions (if the voltage delivered is higher than a threshold, which is typically 1V for water). These reactions induce physical and chemical changes, such as local heating and pH changes, which may cause tissue damage. These adverse effects limit the amount of EStim energy (intensity \times duration) that can be delivered using these electrical circuits, and thus their therapeutic efficacy. In addition, most electrical circuits are prepared with rigid materials, while most biological tissues are soft. This mechanical mismatch can cause tissue injury, inflammation and scar tissue formation, especially when long-term EStim is required. Therefore, there is a critical need for a new generation of electrical circuits capable of conducting ion currents and matching the stiffness of biological tissues to allow delivering higher EStim energy without causing tissue damage.

Some efforts have been undertaken to minimize device-tissue mismatch by pursuing alternative materials and circuit designs. The recently developed ionic conductors are prepared with tissue-matching soft hydrogels infused with salt solutions (177-180) (Figure 8A). Their ion current-conducting capability could potentially eliminate the electrochemical reactions and the associated adverse effects during EStim. However, these ionic conductors lack stability in aqueous environments due to ion diffusion. As a result, they are not suitable for devices that directly interface with biological tissues. To address the issue with ionic conductors, a water-stable, hydrogel-based circuit system, referred to as hydrogel ionic circuit, was developed. Hydrogel ionic circuit is capable of conducting ion currents in its high-concentration salt solution-filled channels (181) (Figure 8B). These salt solution channels are fabricated within a polyethylene glycol (PEG) hydrogel matrix. A unique

aqueous two-phase system formed between the PEG hydrogel and the salt solution stabilizes salt ions in the channels so their diffusion into the PEG hydrogel or the surrounding aqueous medium is minimal. Meanwhile, PEG hydrogels permits ion currents to pass, so EStim can be delivered to biological tissues. These hydrogel ionic circuits have been used to deliver EStim to induce muscle contraction. Adverse effects associated with EStim, including local heating and pH changes are reduced compared to conventional electrodes.

6. Conclusion

EStim holds great therapeutic potentials due to its capability to non-invasively and non-pharmacologically affect cellular activities and biomolecule transport. To address the current issue of inconsistent and inconclusive therapeutic efficacy of EStim, future research on fundamental mechanism of cellular response to EStim needs to be conducted, which will shed light on the optimization of EStim conditions for different applications. New EStim devices will need to be developed to match the properties of biological tissues to maximize EStim delivery capacity while minimizing tissue damages. Additional functions can be added, such as wireless energy transfer, preprogrammed/on-demand EStim to improve the usefulness of the EStim therapy and the patient compliance.

Acknowledgements:

S. Zhao thanks the Research Start-Up Funds from the University of Nebraska Medical Center for support of this work. The work in M. Zhao lab was supported by National Institutes of Health (NIH), National Eye Institute Grant EY019101, U.S. Air Force Office of Scientific Research (AFOSR) Multidisciplinary University Research Initiatives (MURI) Grant FA9550-16-1-0052, and Karen Burns Cornea Research fund.

References

1. Gratieri T, Santer V, Kalia YN. Basic principles and current status of transcorneal and transscleral iontophoresis. *Expert Opin Drug Deliv.* 2017;14(9):1091–102. Epub 2016/11/29. doi: 10.1080/17425247.2017.1266334. PubMed PMID: 27892757. [PubMed: 27892757]
2. Balint R, Cassidy NJ, Cartmell SH. Electrical stimulation: a novel tool for tissue engineering. *Tissue Eng Part B Rev.* 2013;19(1):48–57. Epub 2012/08/10. doi: 10.1089/ten.TEB.2012.0183. PubMed PMID: 22873689. [PubMed: 22873689]
3. Gordon T. Electrical Stimulation to Enhance Axon Regeneration After Peripheral Nerve Injuries in Animal Models and Humans. *Neurotherapeutics.* 2016;13(2):295–310. Epub 2016/01/13. doi: 10.1007/s13311-015-0415-1. PubMed PMID: 26754579; PMCID: PMC4824030. [PubMed: 26754579]
4. Love MR, Palee S, Chattipakorn SC, Chattipakorn N. Effects of electrical stimulation on cell proliferation and apoptosis. *J Cell Physiol.* 2018;233(3):1860–76. Epub 2017/04/30. doi: 10.1002/jcp.25975. PubMed PMID: 28452188. [PubMed: 28452188]
5. Ghasemi-Mobarakeh L, Prabhakaran MP, Morshed M, Nasr-Esfahani MH, Baharvand H, Kiani S, Al-Deyab SS, Ramakrishna S. Application of conductive polymers, scaffolds and electrical stimulation for nerve tissue engineering. *J Tissue Eng Regen Med.* 2011;5(4):e17–35. Epub 2011/03/18. doi: 10.1002/term.383. PubMed PMID: 21413155. [PubMed: 21413155]
6. Pedrotty DM, Koh J, Davis BH, Taylor DA, Wolf P, Niklason LE. Engineering skeletal myoblasts: roles of three-dimensional culture and electrical stimulation. *Am J Physiol Heart Circ Physiol.* 2005;288(4):H1620–6. Epub 2004/11/20. doi: 10.1152/ajpheart.00610.2003. PubMed PMID: 15550526. [PubMed: 15550526]
7. Koning M, Harmsen MC, van Luyn MJ, Werker PM. Current opportunities and challenges in skeletal muscle tissue engineering. *J Tissue Eng Regen Med.* 2009;3(6):407–15. Epub 2009/07/04. doi: 10.1002/term.190. PubMed PMID: 19575392. [PubMed: 19575392]

8. Bach AD, Beier JP, Stern-Staeter J, Horch RE. Skeletal muscle tissue engineering. *J Cell Mol Med*. 2004;8(4):413–22. Epub 2004/12/17. doi: 10.1111/j.1582-4934.2004.tb00466.x. PubMed PMID: 15601570; PMCID: PMC6740234. [PubMed: 15601570]
9. Stoppel WL, Kaplan DL, Black LD 3rd. Electrical and mechanical stimulation of cardiac cells and tissue constructs. *Adv Drug Deliv Rev*. 2016;96:135–55. Epub 2015/08/02. doi: 10.1016/j.addr.2015.07.009. PubMed PMID: 26232525; PMCID: PMC4698182. [PubMed: 26232525]
10. Victoria G, Petrisor B, Drew B, Dick D. Bone stimulation for fracture healing: What's all the fuss? *Indian J Orthop*. 2009;43(2):117–20. Epub 2009/10/20. doi: 10.4103/0019-5413.50844. PubMed PMID: 19838359; PMCID: PMC2762251. [PubMed: 19838359]
11. Griffin M, Bayat A. Electrical stimulation in bone healing: critical analysis by evaluating levels of evidence. *Eplasty*. 2011;11:e34. Epub 2011/08/19. PubMed PMID: 21847434; PMCID: PMC3145421. [PubMed: 21847434]
12. Leppik L, Zhihua H, Mobini S, Thottakkattumana Parameswaran V, Eischen-Loges M, Slavici A, Helbing J, Pindur L, Oliveira KMC, Bhavsar MB, Hudak L, Henrich D, Barker JH. Combining electrical stimulation and tissue engineering to treat large bone defects in a rat model. *Sci Rep*. 2018;8(1):6307. Epub 2018/04/22. doi: 10.1038/s41598-018-24892-0. PubMed PMID: 29679025; PMCID: PMC5910383. [PubMed: 29679025]
13. Thakral G, Lafontaine J, Najafi B, Talal TK, Kim P, Lavery LA. Electrical stimulation to accelerate wound healing. *Diabet Foot Ankle*. 2013;4. Epub 2013/09/21. doi: 10.3402/dfa.v4i0.22081. PubMed PMID: 24049559; PMCID: PMC3776323.
14. Zhao M, Song B, Pu J, Wada T, Reid B, Tai G, Wang F, Guo A, Walczysko P, Gu Y, Sasaki T, Suzuki A, Forrester JV, Bourne HR, Devreotes PN, McCaig CD, Penninger JM. Electrical signals control wound healing through phosphatidylinositol-3-OH kinase-gamma and PTEN. *Nature*. 2006;442(7101):457–60. Epub 2006/07/28. doi: 10.1038/nature04925. PubMed PMID: 16871217. [PubMed: 16871217]
15. Zhao M. Electrical fields in wound healing—An overriding signal that directs cell migration. *Semin Cell Dev Biol*. 2009;20(6):674–82. doi: 10.1016/j.semcdb.2008.12.009. PubMed PMID: 19146969. [PubMed: 19146969]
16. Kroeling P, Gross A, Graham N, Burnie SJ, Szeto G, Goldsmith CH, Haines T, Forget M. Electrotherapy for neck pain. *Cochrane Database Syst Rev*. 2013(8):CD004251. Epub 2013/08/28. doi: 10.1002/14651858.CD004251.pub5. PubMed PMID: 23979926. [PubMed: 23979926]
17. Sbruzzi G, Silveira SA, Silva DV, Coronel CC, Plentz RD. Transcutaneous electrical nerve stimulation after thoracic surgery: systematic review and meta-analysis of 11 randomized trials. *Rev Bras Cir Cardiovasc*. 2012;27(1):75–87. Epub 2012/06/26. doi: 10.5935/1678-9741.20120012. PubMed PMID: 22729304. [PubMed: 22729304]
18. Hurlow A, Bennett MI, Robb KA, Johnson MI, Simpson KH, Oxberry SG. Transcutaneous electric nerve stimulation (TENS) for cancer pain in adults. *Cochrane Database Syst Rev*. 2012(3):CD006276. doi: 10.1002/14651858.CD006276.pub3. PubMed PMID: 22419313. [PubMed: 22419313]
19. Claydon LS, Chesterton LS. Does transcutaneous electrical nerve stimulation (TENS) produce 'dose-responses'? A review of systematic reviews on chronic pain. *Physical Therapy Reviews*. 2008;13(6):450–63.
20. Nnoaham KE, Kumbang J. Transcutaneous electrical nerve stimulation (TENS) for chronic pain. *Cochrane Database Syst Rev*. 2008(3):CD003222. Epub 2008/07/23. doi: 10.1002/14651858.CD003222.pub2. PubMed PMID: 18646088. [PubMed: 18646088]
21. Jin DM, Xu Y, Geng DF, Yan TB. Effect of transcutaneous electrical nerve stimulation on symptomatic diabetic peripheral neuropathy: a meta-analysis of randomized controlled trials. *Diabetes Res Clin Pract*. 2010;89(1):10–5. Epub 2010/06/01. doi: 10.1016/j.diabres.2010.03.021. PubMed PMID: 20510476. [PubMed: 20510476]
22. Bjordal JM, Johnson MI, Lopes-Martins RA, Bogen B, Chow R, Ljunggren AE. Short-term efficacy of physical interventions in osteoarthritic knee pain. A systematic review and meta-analysis of randomised placebo-controlled trials. *BMC Musculoskelet Disord*. 2007;8:51. Epub 2007/06/26. doi: 10.1186/1471-2474-8-51. PubMed PMID: 17587446; PMCID: PMC1931596. [PubMed: 17587446]

23. Johnson M, Martinson M. Efficacy of electrical nerve stimulation for chronic musculoskeletal pain: a meta-analysis of randomized controlled trials. *Pain*. 2007;130(1-2):157–65. Epub 2007/03/27. doi: 10.1016/j.pain.2007.02.007. PubMed PMID: 17383095. [PubMed: 17383095]
24. Lake DA. Neuromuscular electrical stimulation. An overview and its application in the treatment of sports injuries. *Sports Med*. 1992;13(5):320–36. Epub 1992/05/01. doi: 10.2165/00007256-199213050-00003. PubMed PMID: 1565927. [PubMed: 1565927]
25. Benninger DH, Lomarev M, Lopez G, Wassermann EM, Li X, Considine E, Hallett M. Transcranial direct current stimulation for the treatment of Parkinson's disease. *J Neurol Neurosurg Psychiatry*. 2010;81(10):1105–11. Epub 2010/09/28. doi: 10.1136/jnnp.2009.202556. PubMed PMID: 20870863; PMCID: PMC4162743. [PubMed: 20870863]
26. Fridriksson J, Rorden C, Elm J, Sen S, George MS, Bonilha L. Transcranial Direct Current Stimulation vs Sham Stimulation to Treat Aphasia After Stroke: A Randomized Clinical Trial. *JAMA Neurol*. 2018;75(12):1470–6. Epub 2018/08/22. doi: 10.1001/jamaneurol.2018.2287. PubMed PMID: 30128538. [PubMed: 30128538]
27. Ferrucci R, Vergari M, Cogiamanian F, Bocci T, Ciocca M, Tomasini E, De Riz M, Scarpini E, Priori A. Transcranial direct current stimulation (tDCS) for fatigue in multiple sclerosis. *NeuroRehabilitation*. 2014;34(1):121–7. Epub 2013/11/29. doi: 10.3233/NRE-131019. PubMed PMID: 24284464. [PubMed: 24284464]
28. San-Juan D, Sarmiento CI, Gonzalez KM, Orenday Barraza JM. Successful Treatment of a Drug-Resistant Epilepsy by Long-term Transcranial Direct Current Stimulation: A Case Report. *Front Neurol*. 2018;9:65. Epub 2018/02/27. doi: 10.3389/fneur.2018.00065. PubMed PMID: 29479337; PMCID: PMC5811469. [PubMed: 29479337]
29. Bystad M, Gronli O, Rasmussen ID, Gundersen N, Nordvang L, Wang-Iversen H, Aslaksen PM. Transcranial direct current stimulation as a memory enhancer in patients with Alzheimer's disease: a randomized, placebo-controlled trial. *Alzheimers Res Ther*. 2016;8(1):13. Epub 2016/03/24. doi: 10.1186/s13195-016-0180-3. PubMed PMID: 27005937; PMCID: PMC4804486. [PubMed: 27005937]
30. Shekhawat GS, Vanneste S. Optimization of Transcranial Direct Current Stimulation of Dorsolateral Prefrontal Cortex for Tinnitus: A Non-Linear Dose-Response Effect. *Sci Rep*. 2018;8(1):8311. Epub 2018/05/31. doi: 10.1038/s41598-018-26665-1. PubMed PMID: 29844532; PMCID: PMC5974180. [PubMed: 29844532]
31. Sampaio-Junior B, Tortella G, Borrione L, Moffa AH, Machado-Vieira R, Cretaz E, Fernandes da Silva A, Fraguas R, Aparicio LV, Klein I, Lafer B, Goerigk S, Bensenor IM, Lotufo PA, Gattaz WF, Brunoni AR. Efficacy and Safety of Transcranial Direct Current Stimulation as an Add-on Treatment for Bipolar Depression: A Randomized Clinical Trial. *JAMA Psychiatry*. 2018;75(2):158–66. Epub 2017/12/29. doi: 10.1001/jamapsychiatry.2017.4040. PubMed PMID: 29282470; PMCID: PMC5838572. [PubMed: 29282470]
32. da Silva MC, Conti CL, Klauss J, Alves LG, do Nascimento Cavalcante HM, Fregni F, Nitsche MA, Nakamura-Palacios EM. Behavioral effects of transcranial direct current stimulation (tDCS) induced dorsolateral prefrontal cortex plasticity in alcohol dependence. *J Physiol Paris*. 2013;107(6):493–502. Epub 2013/07/31. doi: 10.1016/j.jphysparis.2013.07.003. PubMed PMID: 23891741. [PubMed: 23891741]
33. Lefaucheur JP, Antal A, Ayache SS, Benninger DH, Brunelin J, Cogiamanian F, Cotelli M, De Ridder D, Ferrucci R, Langguth B, Marangolo P, Mylius V, Nitsche MA, Padberg F, Palm U, Poulet E, Priori A, Rossi S, Schecklmann M, Vanneste S, Ziemann U, Garcia-Larrea L, Paulus W. Evidence-based guidelines on the therapeutic use of transcranial direct current stimulation (tDCS). *Clin Neurophysiol*. 2017;128(1):56–92. Epub 2016/11/21. doi: 10.1016/j.clinph.2016.10.087. PubMed PMID: 27866120. [PubMed: 27866120]
34. Panus PC, Campbell J, Kulkarni SB, Herrick RT, Ravis WR, Banga AK. Transdermal iontophoretic delivery of ketoprofen through human cadaver skin and in humans. *Journal of Controlled Release*. 1997;44(2):113–21. doi: 10.1016/S0168-3659(96)01509-X.
35. Labala S, Jose A, Venuganti VVK. Transcutaneous iontophoretic delivery of STAT3 siRNA using layer-by-layer chitosan coated gold nanoparticles to treat melanoma. *Colloids and Surfaces B: Biointerfaces*. 2016;146:188–97. doi: 10.1016/j.colsurfb.2016.05.076. [PubMed: 27318964]

36. Bernardi DS, Bitencourt C, da Silveira DSC, da Cruz ELCM, Pereira-da-Silva MA, Faccioli LH, Lopez RFV. Effective transcutaneous immunization using a combination of iontophoresis and nanoparticles. *Nanomedicine: Nanotechnology, Biology and Medicine*. 2016;12(8):2439–48. doi: 10.1016/j.nano.2016.07.001.
37. Doucet BM, Lam A, Griffin L. Neuromuscular electrical stimulation for skeletal muscle function. *Yale J Biol Med*. 2012;85(2):201–15. Epub 2012/06/28. PubMed PMID: 22737049; PMCID: PMC3375668. [PubMed: 22737049]
38. Kern H, Carraro U, Adami N, Biral D, Hofer C, Forstner C, Modlin M, Vogelauer M, Pond A, Boncompagni S, Paolini C, Mayr W, Protasi F, Zampieri S. Home-based functional electrical stimulation rescues permanently denervated muscles in paraplegic patients with complete lower motor neuron lesion. *Neurorehabil Neural Repair*. 2010;24(8):709–21. Epub 2010/05/13. doi: 10.1177/1545968310366129. PubMed PMID: 20460493. [PubMed: 20460493]
39. Johnson M Transcutaneous Electrical Nerve Stimulation: Mechanisms, Clinical Application and Evidence. *Rev Pain*. 2007;1(1):7–11. Epub 2007/08/01. doi: 10.1177/204946370700100103. PubMed PMID: 26526976; PMCID: PMC4589923. [PubMed: 26526976]
40. Tandon N, Cannizzaro C, Chao PH, Maidhof R, Marsano A, Au HT, Radisic M, Vunjak-Novakovic G. Electrical stimulation systems for cardiac tissue engineering. *Nat Protoc*. 2009;4(2):155–73. Epub 2009/01/31. doi: 10.1038/nprot.2008.183. PubMed PMID: 19180087; PMCID: PMC2775058. [PubMed: 19180087]
41. Feiner R, Engel L, Fleischer S, Malki M, Gal I, Shapira A, Shacham-Diamand Y, Dvir T. Engineered hybrid cardiac patches with multifunctional electronics for online monitoring and regulation of tissue function. *Nat Mater*. 2016;15(6):679–85. Epub 2016/03/15. doi: 10.1038/nmat4590. PubMed PMID: 26974408; PMCID: PMC4900449. [PubMed: 26974408]
42. Ahadian S, Ramon-Azcon J, Ostrovidov S, Camci-Unal G, Hosseini V, Kaji H, Ino K, Shiku H, Khademhosseini A, Matsue T. Interdigitated array of Pt electrodes for electrical stimulation and engineering of aligned muscle tissue. *Lab Chip*. 2012;12(18):3491–503. Epub 2012/08/01. doi: 10.1039/c2lc40479f. PubMed PMID: 22847280. [PubMed: 22847280]
43. Koo J, MacEwan MR, Kang SK, Won SM, Stephen M, Gamble P, Xie Z, Yan Y, Chen YY, Shin J, Birenbaum N, Chung S, Kim SB, Khalifeh J, Harburg DV, Bean K, Paskett M, Kim J, Zohny ZS, Lee SM, Zhang R, Luo K, Ji B, Banks A, Lee HM, Huang Y, Ray WZ, Rogers JA. Wireless bioresorbable electronic system enables sustained nonpharmacological neuroregenerative therapy. *Nat Med*. 2018;24(12):1830–6. Epub 2018/10/10. doi: 10.1038/s41591-018-0196-2. PubMed PMID: 30297910. [PubMed: 30297910]
44. Xu B, Akhtar A, Liu Y, Chen H, Yeo WH, Park SI, Boyce B, Kim H, Yu J, Lai HY, Jung S, Zhou Y, Kim J, Cho S, Huang Y, Bretl T, Rogers JA. An epidermal stimulation and sensing platform for sensorimotor prosthetic control, management of lower back exertion, and electrical muscle activation. *Adv Mater*. 2016;28(22):4462–71. doi: 10.1002/adma.201504155. PubMed PMID: 26469201; PMCID: PMC4833675. [PubMed: 26469201]
45. Lee HU, Blasiak A, Agrawal DR, Loong DTB, Thakor NV, All AH, Ho JS, Yang IH. Subcellular electrical stimulation of neurons enhances the myelination of axons by oligodendrocytes. *PLoS one*. 2017;12(7):e0179642–e. doi: 10.1371/journal.pone.0179642. PubMed PMID: 28671962. [PubMed: 28671962]
46. Iwasa SN, Rashidi A, Sefton E, Liu NX, Popovic MR, Morshead CM. Charge-Balanced Electrical Stimulation Can Modulate Neural Precursor Cell Migration in the Presence of Endogenous Electric Fields in Mouse Brains. *eneuro*. 2019;ENEURO.0382–19.2019. doi: 10.1523/ENEURO.0382-19.2019.
47. Hu M, Hong L, Liu C, Hong S, He S, Zhou M, Huang G, Chen Q. Electrical stimulation enhances neuronal cell activity mediated by Schwann cell derived exosomes. *Scientific Reports*. 2019;9(1):4206. doi: 10.1038/s41598-019-41007-5. [PubMed: 30862846]
48. Gordon T, Amirjani N, Edwards DC, Chan KM. Brief post-surgical electrical stimulation accelerates axon regeneration and muscle reinnervation without affecting the functional measures in carpal tunnel syndrome patients. *Experimental Neurology*. 2010;223(1):192–202. doi: 10.1016/j.expneurol.2009.09.020. [PubMed: 19800329]

49. Gordon T, Sulaiman OAR, Ladak A. Chapter 24 Electrical Stimulation for Improving Nerve Regeneration: Where do we Stand? *International Review of Neurobiology*: Academic Press; 2009. p. 433–44.
50. Zeighami A, Alizadeh F, Saviz M. Optimal currents for electrical stimulation of bone fracture repair: A computational analysis including variations in frequency, tissue properties, and fracture morphology. *Bioelectromagnetics*. 2019;40(2):128–35. doi: 10.1002/bem.22173. [PubMed: 30830978]
51. Portan DV, Deligianni DD, Papanicolaou GC, Kostopoulos V, Psarras GC, Tyllianakis M. Combined Optimized Effect of a Highly Self-Organized Nanosubstrate and an Electric Field on Osteoblast Bone Cells Activity. *Biomed Res Int*. 2019;2019:7574635. doi: 10.1155/2019/7574635. PubMed PMID: 31016196; PMCID: 6448337. [PubMed: 31016196]
52. Su C-Y, Fang T, Fang H-W. Effects of Electrostatic Field on Osteoblast Cells for Bone Regeneration Applications. *Biomed Res Int*. 2017;2017:7124817-. Epub 11/13. doi: 10.1155/2017/7124817. PubMed PMID: 29259985.
53. Eischen-Loges M, Oliveira KMC, Bhavsar MB, Barker JH, Leppik L. Pretreating mesenchymal stem cells with electrical stimulation causes sustained long-lasting pro-osteogenic effects. *PeerJ*. 2018;6:e4959. Epub 2018/06/19. doi: 10.7717/peerj.4959. PubMed PMID: 29910982; PMCID: PMC6001709. [PubMed: 29910982]
54. Vadlamani RA, Nie Y, Detwiler DA, Dhanabal A, Kraft AM, Kuang S, Gavin TP, Garner AL. Nanosecond pulsed electric field induced proliferation and differentiation of osteoblasts and myoblasts. *J R Soc Interface*. 2019;16(155):20190079. doi: 10.1098/rsif.2019.0079. PubMed PMID: 31213169; PMCID: 6597781. [PubMed: 31213169]
55. Nagamine K, Sato H, Kai H, Kaji H, Kanzaki M, Nishizawa M. Contractile Skeletal Muscle Cells Cultured with a Conducting Soft Wire for Effective, Selective Stimulation. *Scientific Reports*. 2018;8(1):2253. doi: 10.1038/s41598-018-20729-y. [PubMed: 29396483]
56. Naskar S, Basu B, Kumaran V. Experimental analysis of effect of electric field on mouse myoblast cells using high throughput microfluidic bioreactor. 10th World Biomaterials Congress; 17 May - 22 May, 2016; Montréal, Canada2016.
57. Li L, Gu W, Du J, Reid B, Deng X, Liu Z, Zong Z, Wang H, Yao B, Yang C, Yan J, Zeng L, Chalmers L, Zhao M, Jiang J. Electric fields guide migration of epidermal stem cells and promote skin wound healing. *Wound Repair and Regeneration*. 2012;20(6):840–51. doi: 10.1111/j.1524-475X.2012.00829.x. [PubMed: 23082865]
58. Oliveira KMC, Barker JH, Berezhikov E, Pindur L, Kynigopoulos S, Eischen-Loges M, Han Z, Bhavsar MB, Henrich D, Leppik L. Electrical stimulation shifts healing/scarring towards regeneration in a rat limb amputation model. *Scientific Reports*. 2019;9(1):11433. doi: 10.1038/s41598-019-47389-w. [PubMed: 31391536]
59. Hu W, Wei X, Zhu L, Yin D, Wei A, Bi X, Liu T, Zhou G, Qiang Y, Sun X, Wen Z, Pan Y. Enhancing proliferation and migration of fibroblast cells by electric stimulation based on triboelectric nanogenerator. *Nano Energy*. 2019;57:600–7. doi: 10.1016/j.nanoen.2018.12.077.
60. Pollack GH. The role of aqueous interfaces in the cell. *Advances in Colloid and Interface Science*. 2003;103(2):173–96. doi: 10.1016/S0001-8686(02)00095-7. [PubMed: 12706554]
61. Pollack GH, Reitz FB. Phase transitions and molecular motion in the cell. *Cellular and molecular biology*. 2001;47(5):885–900. PubMed PMID: 11728101. [PubMed: 11728101]
62. Kay AR. How Cells Can Control Their Size by Pumping Ions. *Frontiers in Cell and Developmental Biology*. 2017;5:41. [PubMed: 28534026]
63. Huang L, Cormie P, Messerli MA, Robinson KR. The involvement of Ca²⁺ and integrins in directional responses of zebrafish keratocytes to electric fields. *Journal of Cellular Physiology*. 2009;219(1):162–72. doi: 10.1002/jcp.21660. [PubMed: 19097066]
64. McLaughlin S, Poo MM. The role of electro-osmosis in the electric-field-induced movement of charged macromolecules on the surfaces of cells. *Biophys J*. 1981;34(1):85–93. doi: 10.1016/S0006-3495(81)84838-2. PubMed PMID: 6894257. [PubMed: 6894257]
65. Andreev VP. Cytoplasmic electric fields and electroosmosis: possible solution for the paradoxes of the intracellular transport of biomolecules. *PLoS one*. 2013;8(4):e61884-e. doi: 10.1371/journal.pone.0061884. PubMed PMID: 23613967. [PubMed: 23613967]

66. Schwartz L, da Veiga Moreira J, Jolicoeur M. Physical forces modulate cell differentiation and proliferation processes. *J Cell Mol Med*. 2018;22(2):738–45. Epub 11/30. doi: 10.1111/jcmm.13417. PubMed PMID: 29193856. [PubMed: 29193856]
67. Rico-Varela J, Ho D, Wan LQ. In Vitro Microscale Models for Embryogenesis. *Adv Biosyst*. 2018;2(6):1700235. Epub 05/07. doi: 10.1002/adbi.201700235. PubMed PMID: 30533517. [PubMed: 30533517]
68. Gao R-C, Zhang X-D, Sun Y-H, Kamimura Y, Mogilner A, Devreotes PN, Zhao M. Different roles of membrane potentials in electrotaxis and chemotaxis of dictyostelium cells. *Eukaryot Cell*. 2011;10(9):1251–6. Epub 07/08. doi: 10.1128/EC.05066-11. PubMed PMID: 21743003. [PubMed: 21743003]
69. Nakajima K-I, Zhu K, Sun Y-H, Hegyi B, Zeng Q, Murphy CJ, Small JV, Chen-Izu Y, Izumiya Y, Penninger JM, Zhao M. KCNJ15/Kir4.2 couples with polyamines to sense weak extracellular electric fields in galvanotaxis. *Nature communications*. 2015;6:8532-. doi: 10.1038/ncomms9532. PubMed PMID: 26449415.
70. Nakajima KI, Zhu K, Sun YH, Hegyi B, Zeng Q, Murphy CJ, Small JV, Chen-Izu Y, Izumiya Y, Penninger JM, Zhao M. KCNJ15/Kir4.2 couples with polyamines to sense weak extracellular electric fields in galvanotaxis. *Nat Commun*. 2015;6:8532. Epub 2015/10/10. doi: 10.1038/ncomms9532. PubMed PMID: 26449415; PMCID: PMC4603535. [PubMed: 26449415]
71. Humphries J, Xiong L, Liu J, Prindle A, Yuan F, Arjes HA, Tsimring L, Süel GM. Species-Independent Attraction to Biofilms through Electrical Signaling. *Cell*. 2017;168(1):200–9.e12. doi: 10.1016/j.cell.2016.12.014. [PubMed: 28086091]
72. Borgens RB, Vanable JW Jr., Jaffe LF. Bioelectricity and regeneration: large currents leave the stumps of regenerating newt limbs. *Proc Natl Acad Sci U S A*. 1977;74(10):4528–32. doi: 10.1073/pnas.74.10.4528. PubMed PMID: 270701. [PubMed: 270701]
73. Franklin BM, Voss SR, Osborn JL. Ion channel signaling influences cellular proliferation and phagocyte activity during axolotl tail regeneration. *Mech Dev*. 2017;146:42–54. Epub 06/07. doi: 10.1016/j.mod.2017.06.001. PubMed PMID: 28603004. [PubMed: 28603004]
74. Dahal GR, Pradhan SJ, Bates EA. Inwardly rectifying potassium channels influence *Drosophila* wing morphogenesis by regulating Dpp release. *Development (Cambridge, England)*. 2017;144(15):2771–83. doi: 10.1242/dev.146647. PubMed PMID: 28684627.
75. Sahu A, Ghosh R, Deshpande G, Prasad M. A Gap Junction Protein, *Inx2*, Modulates Calcium Flux to Specify Border Cell Fate during *Drosophila* oogenesis. *PLOS Genetics*. 2017;13(1):e1006542. doi: 10.1371/journal.pgen.1006542. [PubMed: 28114410]
76. Richard M, Hoch M. *Drosophila* eye size is determined by Innexin 2-dependent Decapentaplegic signalling. *Developmental Biology*. 2015;408(1):26–40. doi: 10.1016/j.ydbio.2015.10.011. [PubMed: 26455410]
77. Bates EA. A potential molecular target for morphological defects of fetal alcohol syndrome: Kir2.1. *Current Opinion in Genetics & Development*. 2013;23(3):324–9. doi: 10.1016/j.gde.2013.05.001. [PubMed: 23756044]
78. Bayir E, Sendemir A, Missirlis YF. Mechanobiology of cells and cell systems, such as organoids. *Biophysical reviews*. 2019. doi: 10.1007/s12551-019-00590-7. PubMed PMID: 31502190.
79. Pannekoek W-J, de Rooij J, Gloerich M. Force transduction by cadherin adhesions in morphogenesis. *F1000Res*. 2019;8:F1000 Faculty Rev-44. doi: 10.12688/f1000research.18779.1. PubMed PMID: 31327995.
80. Humphrey JD, Dufresne ER, Schwartz MA. Mechanotransduction and extracellular matrix homeostasis. *Nature Reviews Molecular Cell Biology*. 2014;15:802. doi: 10.1038/nrm3896. [PubMed: 25355505]
81. Li R, Baek KI, Chang CC, Zhou B, Hsiai TK. Mechanosensitive Pathways Involved in Cardiovascular Development and Homeostasis in Zebrafish. *Journal of Vascular Research*. 2019. doi: 10.1159/000501883.
82. Finkelstein EI, Chao PH, Hung CT, Bulinski JC. Electric field-induced polarization of charged cell surface proteins does not determine the direction of galvanotaxis. *Cell motility and the cytoskeleton*. 2007;64(11):833–46. doi: 10.1002/cm.20227. PubMed PMID: 17685443. [PubMed: 17685443]

83. Lin B-J, Tsao S-H, Chen A, Hu S-K, Chao L, Chao P-HG. Lipid rafts sense and direct electric field-induced migration. *Proceedings of the National Academy of Sciences of the United States of America*. 2017;114(32):8568–73. Epub 07/24. doi: 10.1073/pnas.1702526114. PubMed PMID: 28739955. [PubMed: 28739955]
84. Zhu K, Takada Y, Nakajima K, Sun Y, Jiang J, Zhang Y, Zeng Q, Takada Y, Zhao M. Expression of integrins to control migration direction of electrotaxis. *The FASEB Journal*. 2019;33(8):9131–41. doi: 10.1096/fj.201802657R. [PubMed: 31116572]
85. Casares D, Escribá PV, Rosselló CA. Membrane Lipid Composition: Effect on Membrane and Organelle Structure, Function and Compartmentalization and Therapeutic Avenues. *Int J Mol Sci*. 2019;20(9):2167. doi: 10.3390/ijms20092167. PubMed PMID: 31052427.
86. Allen Greg M, Mogilner A, Theriot Julie A. Electrophoresis of Cellular Membrane Components Creates the Directional Cue Guiding Keratocyte Galvanotaxis. *Current Biology*. 2013;23(7):560–8. doi: 10.1016/j.cub.2013.02.047. [PubMed: 23541731]
87. Forrester JV, Lois N, Zhao M, McCaig C. The spark of life: the role of electric fields in regulating cell behaviour using the eye as a model system. *Ophthalmic research*. 2007;39(1):4–16. doi: 10.1159/000097901. PubMed PMID: 17164572. [PubMed: 17164572]
88. Mycielska ME, Djamgoz MBA. Cellular mechanisms of direct-current electric field effects: galvanotaxis and metastatic disease. *Journal of Cell Science*. 2004;117(9):1631. doi: 10.1242/jcs.01125. [PubMed: 15075225]
89. Zhao M, Song B, Pu J, Wada T, Reid B, Tai G, Wang F, Guo A, Walczysko P, Gu Y, Sasaki T, Suzuki A, Forrester JV, Bourne HR, Devreotes PN, McCaig CD, Penninger JM. Electrical signals control wound healing through phosphatidylinositol-3-OH kinase- γ and PTEN. *Nature*. 2006;442(7101):457–60. doi: 10.1038/nature04925. [PubMed: 16871217]
90. Zhao MIN, Pu JIN, Forrester JV, McCaig CD. Membrane lipids, EGF receptors, and intracellular signals colocalize and are polarized in epithelial cells moving directionally in a physiological electric field. *The FASEB Journal*. 2002;16(8):857–9. doi: 10.1096/fj.01-0811fje. [PubMed: 11967227]
91. Fang KS, Ionides E, Oster G, Nuccitelli R, Isseroff RR. Epidermal growth factor receptor relocation and kinase activity are necessary for directional migration of keratinocytes in DC electric fields. *Journal of Cell Science*. 1999;112(12):1967. [PubMed: 10341215]
92. Reid B, Zhao M. The Electrical Response to Injury: Molecular Mechanisms and Wound Healing. *Adv Wound Care (New Rochelle)*. 2014;3(2):184–201. doi: 10.1089/wound.2013.0442. PubMed PMID: 24761358. [PubMed: 24761358]
93. McLaughlin KA, Levin M. Bioelectric signaling in regeneration: Mechanisms of ionic controls of growth and form. *Developmental biology*. 2018;433(2):177–89. Epub 12/25. doi: 10.1016/j.ydbio.2017.08.032. PubMed PMID: 29291972. [PubMed: 29291972]
94. Guo L, Li H, Wang Y, Li Z, Albeck J, Zhao M, Qing Q. Controlling ERK Activation Dynamics in Mammary Epithelial Cells with Alternating Electric Fields through Microelectrodes. *Nano Letters*. 2019;19(10):7526–33. doi: 10.1021/acs.nanolett.9b03411. [PubMed: 31487192]
95. Mobini S, Leppik L, Barker JH. Direct current electrical stimulation chamber for treating cells in vitro. *Biotechniques*. 2016;60(2):95–8. Epub 2016/02/05. doi: 10.2144/000114382. PubMed PMID: 26842356. [PubMed: 26842356]
96. Mobini S, Leppik L, Thottakattumana Parameswaran V, Barker JH. In vitro effect of direct current electrical stimulation on rat mesenchymal stem cells. *PeerJ*. 2017;5:e2821. Epub 2017/01/18. doi: 10.7717/peerj.2821. PubMed PMID: 28097053; PMCID: PMC5237370. [PubMed: 28097053]
97. Du J, Zhen G, Chen H, Zhang S, Qing L, Yang X, Lee G, Mao HQ, Jia X. Optimal electrical stimulation boosts stem cell therapy in nerve regeneration. *Biomaterials*. 2018;181:347–59. Epub 2018/08/12. doi: 10.1016/j.biomaterials.2018.07.015. PubMed PMID: 30098570; PMCID: PMC6201278. [PubMed: 30098570]
98. Wu SY, Hou HS, Sun YS, Cheng JY, Lo KY. Correlation between cell migration and reactive oxygen species under electric field stimulation. *Biomicrofluidics*. 2015;9(5):054120. Epub 2015/10/22. doi: 10.1063/1.4932662. PubMed PMID: 26487906; PMCID: PMC4600077. [PubMed: 26487906]

99. Huang CW, Cheng JY, Yen MH, Young TH. Electrotaxis of lung cancer cells in a multiple-electric-field chip. *Biosens Bioelectron.* 2009;24(12):3510–6. Epub 2009/06/06. doi: 10.1016/j.bios.2009.05.001. PubMed PMID: 19497728. [PubMed: 19497728]
100. Zhao S, Zhu K, Zhang Y, Zhu Z, Xu Z, Zhao M, Pan T. ElectroTaxis-on-a-Chip (ETC): an integrated quantitative high-throughput screening platform for electrical field-directed cell migration. *Lab Chip.* 2014;14(22):4398–405. doi: 10.1039/c4lc00745j. PubMed PMID: 25242672; PMCID: PMC4437771. [PubMed: 25242672]
101. Tsai HF, Peng SW, Wu CY, Chang HF, Cheng JY. Electrotaxis of oral squamous cell carcinoma cells in a multiple-electric-field chip with uniform flow field. *Biomicrofluidics.* 2012;6(3):34116. Epub 2012/01/01. doi: 10.1063/1.4749826. PubMed PMID: 24009650; PMCID: PMC3448594. [PubMed: 24009650]
102. Gao R, Zhao S, Jiang X, Sun Y, Zhao S, Gao J, Borleis J, Willard S, Tang M, Cai H, Kamimura Y, Huang Y, Jiang J, Huang Z, Mogilner A, Pan T, Devreotes PN, Zhao M. A large-scale screen reveals genes that mediate electrotaxis in *Dictyostelium discoideum*. *Sci Signal.* 2015;8(378):ra50. doi: 10.1126/scisignal.aab0562. PubMed PMID: 26012633; PMCID: PMC4470479. [PubMed: 26012633]
103. Tandon N, Marsano A, Maidhof R, Wan L, Park H, Vunjak-Novakovic G. Optimization of electrical stimulation parameters for cardiac tissue engineering. *J Tissue Eng Regen Med.* 2011;5(6):e115–25. Epub 2011/05/24. doi: 10.1002/term.377. PubMed PMID: 21604379; PMCID: PMC3117092. [PubMed: 21604379]
104. Hirt MN, Boeddinghaus J, Mitchell A, Schaaf S, Bornchen C, Muller C, Schulz H, Hubner N, Stenzig J, Stoehr A, Neuber C, Eder A, Luther PK, Hansen A, Eschenhagen T. Functional improvement and maturation of rat and human engineered heart tissue by chronic electrical stimulation. *J Mol Cell Cardiol.* 2014;74:151–61. Epub 2014/05/24. doi: 10.1016/j.yjmcc.2014.05.009. PubMed PMID: 24852842. [PubMed: 24852842]
105. Lasher RA, Pahnke AQ, Johnson JM, Sachse FB, Hitchcock RW. Electrical stimulation directs engineered cardiac tissue to an age-matched native phenotype. *J Tissue Eng.* 2012;3(1):2041731412455354. Epub 2012/08/25. doi: 10.1177/2041731412455354. PubMed PMID: 22919458; PMCID: PMC3424978. [PubMed: 22919458]
106. Ghasemi-Mobarakeh L, Prabhakaran MP, Morshed M, Nasr-Esfahani MH, Ramakrishna S. Electrical stimulation of nerve cells using conductive nanofibrous scaffolds for nerve tissue engineering. *Tissue Eng Part A.* 2009;15(11):3605–19. Epub 2009/06/06. doi: 10.1089/ten.TEA.2008.0689. PubMed PMID: 19496678. [PubMed: 19496678]
107. Xie J, Macewan MR, Willerth SM, Li X, Moran DW, Sakiyama-Elbert SE, Xia Y. Conductive Core-Sheath Nanofibers and Their Potential Application in Neural Tissue Engineering. *Adv Funct Mater.* 2009;19(14):2312–8. Epub 2009/10/16. doi: 10.1002/adfm.200801904. PubMed PMID: 19830261; PMCID: PMC2760838. [PubMed: 19830261]
108. Zhang Z, Rouabhia M, Wang Z, Roberge C, Shi G, Roche P, Li J, Dao LH. Electrically conductive biodegradable polymer composite for nerve regeneration: electricity-stimulated neurite outgrowth and axon regeneration. *Artif Organs.* 2007;31(1):13–22. Epub 2007/01/11. doi: 10.1111/j.1525-1594.2007.00335.x. PubMed PMID: 17209956. [PubMed: 17209956]
109. Lee JY, Bashur CA, Goldstein AS, Schmidt CE. Polypyrrole-coated electrospun PLGA nanofibers for neural tissue applications. *Biomaterials.* 2009;30(26):4325–35. Epub 2009/06/09. doi: 10.1016/j.biomaterials.2009.04.042. PubMed PMID: 19501901; PMCID: PMC2713816. [PubMed: 19501901]
110. Huang J, Lu L, Zhang J, Hu X, Zhang Y, Liang W, Wu S, Luo Z. Electrical stimulation to conductive scaffold promotes axonal regeneration and remyelination in a rat model of large nerve defect. *PLoS One.* 2012;7(6):e39526. Epub 2012/06/28. doi: 10.1371/journal.pone.0039526. PubMed PMID: 22737243; PMCID: PMC3380893. [PubMed: 22737243]
111. Gordon T, Udina E, Verge VM, de Chaves EI. Brief electrical stimulation accelerates axon regeneration in the peripheral nervous system and promotes sensory axon regeneration in the central nervous system. *Motor Control.* 2009;13(4):412–41. Epub 2009/12/18. PubMed PMID: 20014648. [PubMed: 20014648]
112. Xu C, Kou Y, Zhang P, Han N, Yin X, Deng J, Chen B, Jiang B. Electrical stimulation promotes regeneration of defective peripheral nerves after delayed repair intervals lasting under one month.

- PLoS One. 2014;9(9):e105045. Epub 2014/09/03. doi: 10.1371/journal.pone.0105045. PubMed PMID: 25181499; PMCID: PMC4152131. [PubMed: 25181499]
113. Banan Sadeghian R, Ebrahimi M, Salehi S. Electrical stimulation of microengineered skeletal muscle tissue: Effect of stimulus parameters on myotube contractility and maturation. *J Tissue Eng Regen Med*. 2018;12(4):912–22. Epub 2017/06/18. doi: 10.1002/term.2502. PubMed PMID: 28622706. [PubMed: 28622706]
 114. Khodabukus A, Madden L, Prabhu NK, Koves TR, Jackman CP, Muoio DM, Bursac N. Electrical stimulation increases hypertrophy and metabolic flux in tissue-engineered human skeletal muscle. *Biomaterials*. 2019;198:259–69. Epub 2018/09/06. doi: 10.1016/j.biomaterials.2018.08.058. PubMed PMID: 30180985; PMCID: PMC6395553. [PubMed: 30180985]
 115. Ito A, Yamamoto Y, Sato M, Ikeda K, Yamamoto M, Fujita H, Nagamori E, Kawabe Y, Kamihira M. Induction of functional tissue-engineered skeletal muscle constructs by defined electrical stimulation. *Sci Rep*. 2014;4:4781. Epub 2014/04/25. doi: 10.1038/srep04781. PubMed PMID: 24759171; PMCID: PMC3998029. [PubMed: 24759171]
 116. Radisic M, Park H, Shing H, Consi T, Schoen FJ, Langer R, Freed LE, Vunjak-Novakovic G. Functional assembly of engineered myocytes by electrical stimulation of cardiac myocytes cultured on scaffolds. *Proc Natl Acad Sci U S A*. 2004;101(52):18129–34. Epub 2004/12/18. doi: 10.1073/pnas.0407817101. PubMed PMID: 15604141; PMCID: PMC539727. [PubMed: 15604141]
 117. Hu WW, Hsu YT, Cheng YC, Li C, Ruaan RC, Chien CC, Chung CA, Tsao CW. Electrical stimulation to promote osteogenesis using conductive polypyrrole films. *Mater Sci Eng C Mater Biol Appl*. 2014;37:28–36. Epub 2014/03/04. doi: 10.1016/j.msec.2013.12.019. PubMed PMID: 24582219. [PubMed: 24582219]
 118. Hu WW, Chen TC, Tsao CW, Cheng YC. The effects of substrate-mediated electrical stimulation on the promotion of osteogenic differentiation and its optimization. *J Biomed Mater Res B Appl Biomater*. 2019;107(5):1607–19. Epub 2018/10/16. doi: 10.1002/jbm.b.34253. PubMed PMID: 30318825. [PubMed: 30318825]
 119. Tandon N, Cannizzaro C, Figallo E, Voldman J, Vunjak-Novakovic G. Characterization of electrical stimulation electrodes for cardiac tissue engineering. *Conf Proc IEEE Eng Med Biol Soc*. 2006;1:845–8. Epub 2007/10/20. doi: 10.1109/IEMBS.2006.259747. PubMed PMID: 17946862.
 120. Balint R, Cassidy NJ, Cartmell SH. Conductive polymers: towards a smart biomaterial for tissue engineering. *Acta Biomater*. 2014;10(6):2341–53. Epub 2014/02/22. doi: 10.1016/j.actbio.2014.02.015. PubMed PMID: 24556448. [PubMed: 24556448]
 121. Gorain B, Choudhury H, Pandey M, Kesharwani P, Abeer MM, Tekade RK, Hussain Z. Carbon nanotube scaffolds as emerging nanoplatform for myocardial tissue regeneration: A review of recent developments and therapeutic implications. *Biomed Pharmacother*. 2018;104:496–508. Epub 2018/05/26. doi: 10.1016/j.biopha.2018.05.066. PubMed PMID: 29800914. [PubMed: 29800914]
 122. Schmidt CE, Shastri VR, Vacanti JP, Langer R. Stimulation of neurite outgrowth using an electrically conducting polymer. *Proc Natl Acad Sci U S A*. 1997;94(17):8948–53. Epub 1997/08/19. doi: 10.1073/pnas.94.17.8948. PubMed PMID: 9256415; PMCID: PMC22977. [PubMed: 9256415]
 123. Li M, Guo Y, Wei Y, MacDiarmid AG, Lelkes PI. Electrospinning polyaniline-contained gelatin nanofibers for tissue engineering applications. *Biomaterials*. 2006;27(13):2705–15. Epub 2005/12/15. doi: 10.1016/j.biomaterials.2005.11.037. PubMed PMID: 16352335. [PubMed: 16352335]
 124. Chen MC, Sun YC, Chen YH. Electrically conductive nanofibers with highly oriented structures and their potential application in skeletal muscle tissue engineering. *Acta Biomater*. 2013;9(3):5562–72. Epub 2012/10/27. doi: 10.1016/j.actbio.2012.10.024. PubMed PMID: 23099301. [PubMed: 23099301]
 125. Cen L, Neoh KG, Kang ET. Surface Functionalization of Electrically Conductive Polypyrrole Film with Hyaluronic Acid. *Langmuir*. 2002;18(22):8633–40.

126. Lee JW, Serna F, Nickels J, Schmidt CE. Carboxylic acid-functionalized conductive polypyrrole as a bioactive platform for cell adhesion. *Biomacromolecules*. 2006;7(6):1692–5. Epub 2006/06/14. doi: 10.1021/bm060220q. PubMed PMID: 16768385; PMCID: PMC2548274. [PubMed: 16768385]
127. Stauffer WR, Cui XT. Polypyrrole doped with 2 peptide sequences from laminin. *Biomaterials*. 2006;27(11):2405–13. Epub 2005/12/14. doi: 10.1016/j.biomaterials.2005.10.024. PubMed PMID: 16343612. [PubMed: 16343612]
128. Veetil JV, Ye K. Tailored carbon nanotubes for tissue engineering applications. *Biotechnol Prog*. 2009;25(3):709–21. Epub 2009/06/06. doi: 10.1002/btpr.165. PubMed PMID: 19496152; PMCID: PMC2700190. [PubMed: 19496152]
129. Mollon B, da Silva V, Busse JW, Einhorn TA, Bhandari M. Electrical stimulation for long-bone fracture-healing: a meta-analysis of randomized controlled trials. *J Bone Joint Surg Am*. 2008;90(11):2322–30. Epub 2008/11/04. doi: 10.2106/JBJS.H.00111. PubMed PMID: 18978400. [PubMed: 18978400]
130. Eberstein A, Eberstein S. Electrical stimulation of denervated muscle: is it worthwhile? *Med Sci Sports Exerc*. 1996;28(12):1463–9. Epub 1996/12/01. PubMed PMID: 8970139. [PubMed: 8970139]
131. Kern H, Hofer C, Strohhofer M, Mayr W, Richter W, Stohr H. Standing up with denervated muscles in humans using functional electrical stimulation. *Artif Organs*. 1999;23(5):447–52. Epub 1999/06/23. doi: 10.1046/j.1525-1594.1999.06376.x. PubMed PMID: 10378940. [PubMed: 10378940]
132. Mortimer JT, Bhadra N. Peripheral nerve and muscle stimulation. In: Horch KW, Dhillon GS, editors. *Series on Bioengineering and Biomedical Engineering: Volume 22004*.
133. Cogan SF, Ludwig KA, Welle CG, Takmakov P. Tissue damage thresholds during therapeutic electrical stimulation. *J Neural Eng*. 2016;13(2):021001. Epub 2016/01/23. doi: 10.1088/1741-2560/13/2/021001. PubMed PMID: 26792176; PMCID: PMC5386002. [PubMed: 26792176]
134. Butterwick A, Vankov A, Huie P, Freyvert Y, Palanker D. Tissue damage by pulsed electrical stimulation. *IEEE Trans Biomed Eng*. 2007;54(12):2261–7. Epub 2007/12/14. doi: 10.1109/tbme.2007.908310. PubMed PMID: 18075042. [PubMed: 18075042]
135. Wong JN, Olson JL, Morhart MJ, Chan KM. Electrical stimulation enhances sensory recovery: a randomized controlled trial. *Ann Neurol*. 2015;77(6):996–1006. Epub 2015/03/03. doi: 10.1002/ana.24397. PubMed PMID: 25727139. [PubMed: 25727139]
136. Gordon T, Amirjani N, Edwards DC, Chan KM. Brief post-surgical electrical stimulation accelerates axon regeneration and muscle reinnervation without affecting the functional measures in carpal tunnel syndrome patients. *Exp Neurol*. 2010;223(1):192–202. Epub 2009/10/06. doi: 10.1016/j.expneurol.2009.09.020. PubMed PMID: 19800329. [PubMed: 19800329]
137. Chan KM, Curran MW, Gordon T. The use of brief post-surgical low frequency electrical stimulation to enhance nerve regeneration in clinical practice. *J Physiol*. 2016;594(13):3553–9. Epub 2016/02/13. doi: 10.1113/JP270892. PubMed PMID: 26864594; PMCID: PMC4929315. [PubMed: 26864594]
138. Vance CG, Dailey DL, Rakel BA, Sluka KA. Using TENS for pain control: the state of the evidence. *Pain Manag*. 2014;4(3):197–209. Epub 2014/06/24. doi: 10.2217/pmt.14.13. PubMed PMID: 24953072; PMCID: PMC4186747. [PubMed: 24953072]
139. Guo X, Jiang X, Ren X, Sun H, Zhang D, Zhang Q, Zhang J, Huang Y. The Galvanotactic Migration of Keratinocytes is Enhanced by Hypoxic Preconditioning. *Sci Rep*. 2015;5:10289. Epub 2015/05/20. doi: 10.1038/srep10289. PubMed PMID: 25988491; PMCID: PMC4437307. [PubMed: 25988491]
140. Ren X, Sun H, Liu J, Guo X, Huang J, Jiang X, Zhang Y, Huang Y, Fan D, Zhang J. Keratinocyte electrotaxis induced by physiological pulsed direct current electric fields. *Bioelectrochemistry*. 2019;127:113–24. Epub 2019/03/01. doi: 10.1016/j.bioelechem.2019.02.001. PubMed PMID: 30818261. [PubMed: 30818261]
141. Kim MS, Lee MH, Kwon BJ, Seo HJ, Koo MA, You KE, Kim D, Park JC. Control of neonatal human dermal fibroblast migration on poly(lactic-co-glycolic acid)-coated surfaces by

- electrotaxis. *J Tissue Eng Regen Med*. 2017;11(3):862–8. Epub 2015/01/30. doi: 10.1002/term.1986. PubMed PMID: 25627750. [PubMed: 25627750]
142. Guo A, Song B, Reid B, Gu Y, Forrester JV, Jahoda CA, Zhao M. Effects of physiological electric fields on migration of human dermal fibroblasts. *J Invest Dermatol*. 2010;130(9):2320–7. Epub 2010/04/23. doi: 10.1038/jid.2010.96. PubMed PMID: 20410911; PMCID: PMC2952177. [PubMed: 20410911]
 143. Peters EJ, Lavery LA, Armstrong DG, Fleischli JG. Electric stimulation as an adjunct to heal diabetic foot ulcers: a randomized clinical trial. *Arch Phys Med Rehabil*. 2001;82(6):721–5. Epub 2001/06/02. doi: 10.1053/apmr.2001.23780. PubMed PMID: 11387573. [PubMed: 11387573]
 144. Wood JM, Evans PE 3rd, Schallreuter KU, Jacobson WE, Sufit R, Newman J, White C, Jacobson M. A multicenter study on the use of pulsed low-intensity direct current for healing chronic stage II and stage III decubitus ulcers. *Arch Dermatol*. 1993;129(8):999–1009. Epub 1993/08/01. PubMed PMID: 8352625. [PubMed: 8352625]
 145. Houghton PE, Campbell KE, Fraser CH, Harris C, Keast DH, Potter PJ, Hayes KC, Woodbury MG. Electrical stimulation therapy increases rate of healing of pressure ulcers in community-dwelling people with spinal cord injury. *Arch Phys Med Rehabil*. 2010;91(5):669–78. Epub 2010/05/04. doi: 10.1016/j.apmr.2009.12.026. PubMed PMID: 20434602. [PubMed: 20434602]
 146. Griffin JW, Tooms RE, Mendi RA, Clift JK, Vander Zwaag R, el-Zeky F. Efficacy of high voltage pulsed current for healing of pressure ulcers in patients with spinal cord injury. *Phys Ther*. 1991;71(6):433–42; discussion 42–4. Epub 1991/06/01. doi: 10.1093/ptj/71.6.433. PubMed PMID: 2034707. [PubMed: 2034707]
 147. Houghton PE, Kincaid CB, Lovell M, Campbell KE, Keast DH, Woodbury MG, Harris KA. Effect of electrical stimulation on chronic leg ulcer size and appearance. *Phys Ther*. 2003;83(1):17–28. Epub 2002/12/24. PubMed PMID: 12495409. [PubMed: 12495409]
 148. Adunsky A, Ohry A, Group D. Decubitus direct current treatment (DDCT) of pressure ulcers: results of a randomized double-blinded placebo controlled study. *Arch Gerontol Geriatr*. 2005;41(3):261–9. Epub 2005/07/07. doi: 10.1016/j.archger.2005.04.004. PubMed PMID: 15998547. [PubMed: 15998547]
 149. Lundeberg TC, Eriksson SV, Malm M. Electrical nerve stimulation improves healing of diabetic ulcers. *Ann Plast Surg*. 1992;29(4):328–31. Epub 1992/10/01. PubMed PMID: 1466529. [PubMed: 1466529]
 150. Carley PJ, Wainapel SF. Electrotherapy for acceleration of wound healing: low intensity direct current. *Arch Phys Med Rehabil*. 1985;66(7):443–6. Epub 1985/07/01. PubMed PMID: 3893385. [PubMed: 3893385]
 151. Jankovic A, Binic I. Frequency rhythmic electrical modulation system in the treatment of chronic painful leg ulcers. *Arch Dermatol Res*. 2008;300(7):377–83. Epub 2008/07/17. doi: 10.1007/s00403-008-0875-9. PubMed PMID: 18629524. [PubMed: 18629524]
 152. Lawson D, Petrofsky JS. A randomized control study on the effect of biphasic electrical stimulation in a warm room on skin blood flow and healing rates in chronic wounds of patients with and without diabetes. *Med Sci Monit*. 2007;13(6):CR258–63. Epub 2007/05/31. PubMed PMID: 17534231.
 153. Feedar JA, Kloth LC, Gentzkow GD. Chronic dermal ulcer healing enhanced with monophasic pulsed electrical stimulation. *Phys Ther*. 1991;71(9):639–49. Epub 1991/09/01. doi: 10.1093/ptj/71.9.639. PubMed PMID: 1881954. [PubMed: 1881954]
 154. Morris C Bio-electrical stimulation therapy using POSiFECT®RD. *Wounds UK*. 2006;2(4):112–6.
 155. Banerjee J, Das Ghatak P, Roy S, Khanna S, Sequin EK, Bellman K, Dickinson BC, Suri P, Subramaniam VV, Chang CJ, Sen CK. Improvement of human keratinocyte migration by a redox active bioelectric dressing. *PLoS One*. 2014;9(3):e89239. Epub 2014/03/07. doi: 10.1371/journal.pone.0089239. PubMed PMID: 24595050; PMCID: PMC3940438. [PubMed: 24595050]
 156. Kim H, Makin I, Skiba J, Ho A, Housler G, Stojadinovic A, Izadjoo M. Antibacterial efficacy testing of a bioelectric wound dressing against clinical wound pathogens. *Open Microbiol J*. 2014;8:15–21. Epub 2014/03/15. doi: 10.2174/1874285801408010015. PubMed PMID: 24627730; PMCID: PMC3950956. [PubMed: 24627730]

157. Leloup P, Toussaint P, Lembelembe JP, Celerier P, Maillard H. The analgesic effect of electrostimulation (WoundEL(R)) in the treatment of leg ulcers. *Int Wound J*. 2015;12(6):706–9. Epub 2014/03/13. doi: 10.1111/iwj.12211. PubMed PMID: 24618089. [PubMed: 24618089]
158. Zhang Y, Chen Y, Yu X, Qi Y, Chen Y, Liu Y, Hu Y, Li Z. A flexible device for ocular iontophoretic drug delivery. *Biomicrofluidics*. 2016;10(1):011911. Epub 2016/03/10. doi: 10.1063/1.4942516. PubMed PMID: 26958098; PMCID: PMC4769262. [PubMed: 26958098]
159. Jung JH, Chiang B, Grossniklaus HE, Prausnitz MR. Ocular drug delivery targeted by iontophoresis in the suprachoroidal space using a microneedle. *J Control Release*. 2018;277:14–22. Epub 2018/03/06. doi: 10.1016/j.jconrel.2018.03.001. PubMed PMID: 29505807; PMCID: PMC5911252. [PubMed: 29505807]
160. Christopher K, Chauhan A. Contact Lens Based Drug Delivery to the Posterior Segment Via Iontophoresis in Cadaver Rabbit Eyes. *Pharm Res*. 2019;36(6):87. Epub 2019/04/21. doi: 10.1007/s11095-019-2625-4. PubMed PMID: 31004227. [PubMed: 31004227]
161. O'Brart DP. Riboflavin for corneal cross-linking. *Drugs Today (Barc)*. 2016;52(6):331–46. Epub 2016/07/28. doi: 10.1358/dot.2016.52.6.2494140. PubMed PMID: 27458610. [PubMed: 27458610]
162. Bikbova G, Bikbov M. Transepithelial corneal collagen cross-linking by iontophoresis of riboflavin. *Acta Ophthalmol*. 2014;92(1):e30–4. Epub 2013/07/16. doi: 10.1111/aos.12235. PubMed PMID: 23848196. [PubMed: 23848196]
163. Bikbova G, Bikbov M. Standard corneal collagen crosslinking versus transepithelial iontophoresis-assisted corneal crosslinking, 24 months follow-up: randomized control trial. *Acta Ophthalmol*. 2016;94(7):e600–e6. Epub 2016/10/19. doi: 10.1111/aos.13032. PubMed PMID: 27040458; PMCID: PMC5111766. [PubMed: 27040458]
164. Patane MA, Cohen A, From S, Torkildsen G, Welch D, Ousler GW 3rd. Ocular iontophoresis of EGP-437 (dexamethasone phosphate) in dry eye patients: results of a randomized clinical trial. *Clin Ophthalmol*. 2011;5:633–43. Epub 2011/06/02. doi: 10.2147/OPTH.S19349. PubMed PMID: 21629568; PMCID: PMC3104791. [PubMed: 21629568]
165. Cohen AE, Assang C, Patane MA, From S, Korenfeld M, Avion Study I. Evaluation of dexamethasone phosphate delivered by ocular iontophoresis for treating noninfectious anterior uveitis. *Ophthalmology*. 2012;119(1):66–73. Epub 2011/11/26. doi: 10.1016/j.jophtha.2011.07.006. PubMed PMID: 22115712. [PubMed: 22115712]
166. Halhal M, Renard G, Courtois Y, BenEzra D, Behar-Cohen F. Iontophoresis: from the lab to the bed side. *Exp Eye Res*. 2004;78(3):751–7. Epub 2004/04/27. PubMed PMID: 15106955. [PubMed: 15106955]
167. Haghjou N, Soheilian M, Abdekhodaie MJ. Sustained release intraocular drug delivery devices for treatment of uveitis. *J Ophthalmic Vis Res*. 2011;6(4):317–29. Epub 2012/03/29. PubMed PMID: 22454753; PMCID: PMC3306122. [PubMed: 22454753]
168. Parkinson TM, Ferguson E, Febraro S, Bakhtyari A, King M, Mundasad M. Tolerance of ocular iontophoresis in healthy volunteers. *J Ocul Pharmacol Ther*. 2003;19(2):145–51. Epub 2003/06/14. doi: 10.1089/108076803321637672. PubMed PMID: 12804059. [PubMed: 12804059]
169. Churchill CDM, Winter P, Tuszyński JA, Levin M. EDEn—Electroceutical Design Environment: Ion Channel Tissue Expression Database with Small Molecule Modulators. *iScience*. 2019;11:42–56. doi: 10.1016/j.isci.2018.12.003. [PubMed: 30590250]
170. Fricke H The Electric Permittivity of a Dilute Suspension of Membrane-Covered Ellipsoids. *Journal of Applied Physics*. 1953;24(5):644–6. doi: 10.1063/1.1721343.
171. Schwan HP. Electrical Properties of Tissue and Cell Suspensions* *This work was supported in part by grants from the United States Public Health Service, H-1253(c2–4) and in part by the Office of Naval Research, 119–289. In: Lawrence JH, Tobias CA, editors. *Advances in Biological and Medical Physics*; Elsevier; 1957. p. 147–209.
172. Meny I, Burais N, Buret F, Nicolas L. Finite-Element Modeling of Cell Exposed to Harmonic and Transient Electric Fields. *IEEE Transactions on Magnetics*. 2007;43(4):1773–6. doi: 10.1109/TMAG.2007.892517.

173. Gowrishankar TR, Smith KC, Weaver JC. Transport-Based Biophysical System Models of Cells for Quantitatively Describing Responses to Electric Fields. *Proceedings of the IEEE*. 2013;101(2):505–17. doi: 10.1109/JPROC.2012.2200289.
174. Schoenbach KH, Joshi RP, Kolb JF, Nianyong C, Stacey M, Blackmore PF, Buescher ES, Beebe SJ. Ultrashort electrical pulses open a new gateway into biological cells. *Proceedings of the IEEE*. 2004;92(7):1122–37. doi: 10.1109/JPROC.2004.829009.
175. Pietak A, Levin M. Exploring Instructive Physiological Signaling with the Bioelectric Tissue Simulation Engine. *Front Bioeng Biotechnol*. 2016;4:55-. doi: 10.3389/fbioe.2016.00055. PubMed PMID: 27458581. [PubMed: 27458581]
176. Newbold C, Richardson R, Millard R, Seligman P, Cowan R, Shepherd R. Electrical stimulation causes rapid changes in electrode impedance of cell-covered electrodes. *J Neural Eng*. 2011;8(3):036029. Epub 2011/05/17. doi: 10.1088/1741-2560/8/3/036029. PubMed PMID: 21572219; PMCID: PMC3147028. [PubMed: 21572219]
177. Keplinger C, Sun JY, Foo CC, Rothemund P, Whitesides GM, Suo Z. Stretchable, transparent, ionic conductors. *Science*. 2013;341(6149):984–7. doi: 10.1126/science.1240228. PubMed PMID: 23990555. [PubMed: 23990555]
178. Sun JY, Keplinger C, Whitesides GM, Suo Z. Ionic skin. *Adv Mater*. 2014;26(45):7608–14. doi: 10.1002/adma.201403441. PubMed PMID: 25355528. [PubMed: 25355528]
179. Yang CH, Chen B, Lu JJ, Yang JH, Zhou J, Chen YM, Suo Z. Ionic cable. *Extreme Mechanics Letters*. 2015;3:59–65.
180. Kim CC, Lee HH, Oh KH, Sun JY. Highly stretchable, transparent ionic touch panel. *Science*. 2016;353(6300):682–7. doi: 10.1126/science.aaf8810. PubMed PMID: 27516597. [PubMed: 27516597]
181. Zhao S, Tseng P, Grasman J, Wang Y, Li W, Napier B, Yavuz B, Chen Y, Howell L, Rincon J, Omenetto FG, Kaplan DL. Programmable Hydrogel Ionic Circuits for Biologically Matched Electronic Interfaces. *Adv Mater*. 2018;30(25):e1800598. Epub 2018/05/03. doi: 10.1002/adma.201800598. PubMed PMID: 29717798. [PubMed: 29717798]

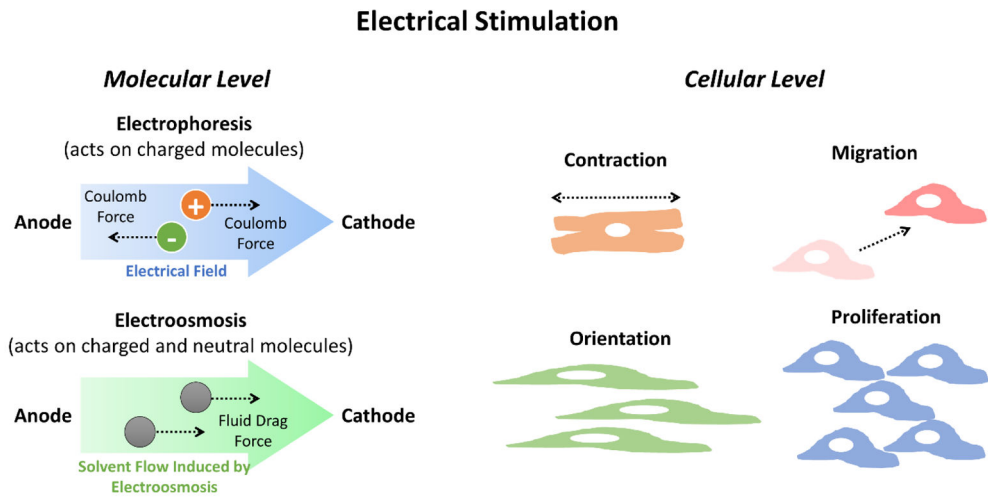


Fig. 1. EStim has multiple effects at molecular and cellular levels

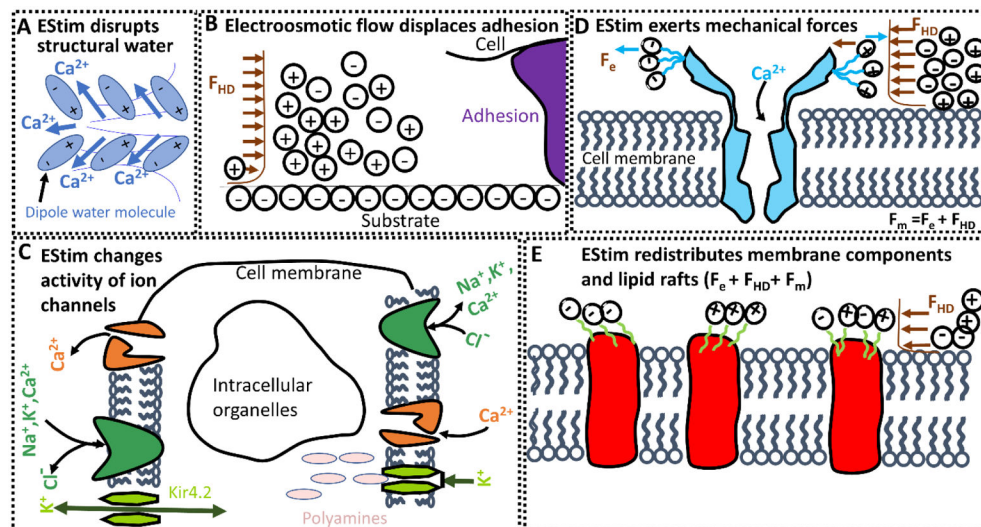


Fig. 2. Models depicting the fundamental physical effects of EStim on cells (A) Application of electrical field disrupts the layer of structured water leading to a calcium wave. Entry of Na⁺ ions and escape of K⁺ ions also take place when layer of structured water is disrupted (not shown in current figure). (B) Hydrodynamic drag force (F_{HD}) on the cell applied by the electroosmotic flow at the charged migration surface could displace adhesions laterally. (C) Polarization of the cell by EStim can change electromotive forces (F_e) and opening/closing of voltage-gated ion channels. (D) Electroosmotic forces (F_{HD}) combine with electrostatic forces (F_e) on charged macromolecules and membrane components produce mechanical forces (F_m). As depicted, this could asymmetrically activate a force sensor creating a local signal that could be used to define the front and the back of the cell. (E) Local electroosmotic (F_{HD}) and electrostatic forces (F_e) at the cell membrane can also push other membrane components. Negatively charged components will move towards the anode, and positively charged components will migrate towards the cathode. Depending upon the net surface charge possessed by the proteins of the cell they will be pushed to one side of the cell or the other as a cause by the electroosmotic forces at the membrane. Similarly, all three forces, electroosmotic (F_{HD}), electrostatic forces (F_e), and mechanical work (F_m) add up to drag lipid rafts towards the cathode.

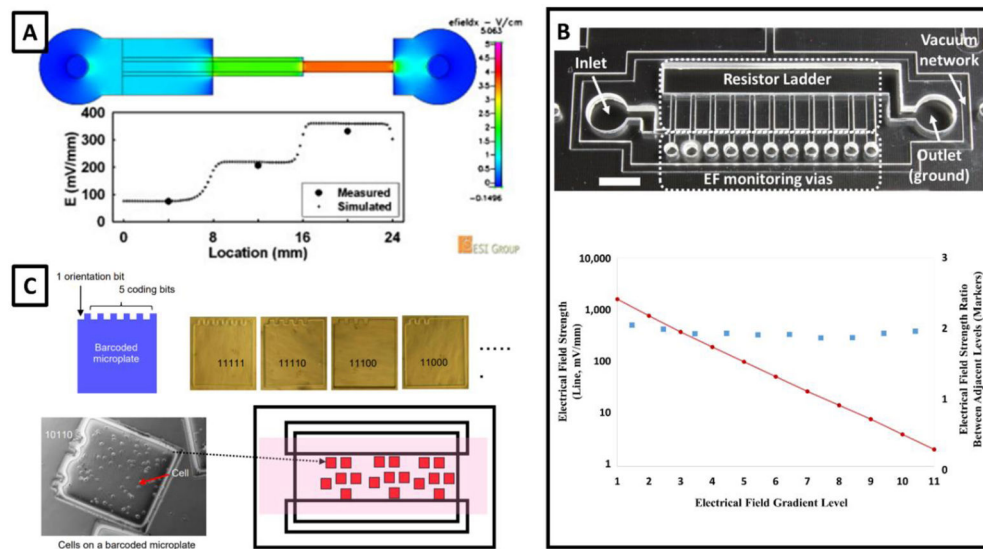


Fig. 3. High-throughput systems for testing cellular responses to EStim. (a) A multi-field microfluidic device that can generate three different electrical field strengths simultaneously. Image reproduced from (99) with permission. Copyright 2009, Elsevier. (b) A resistor ladder-based microfluidic device that can generate 10 levels of electrical field strength spanning over three orders of magnitude. Adapted from (100) with permission. Copyright 2014, Royal Society of Chemistry. (c) A microplate platform that allows testing 30 different *Dictyostelium discoideum* strains in one experiment. Reproduced from (102) with permission. Copyright 2015, American Association for the Advancement of Science

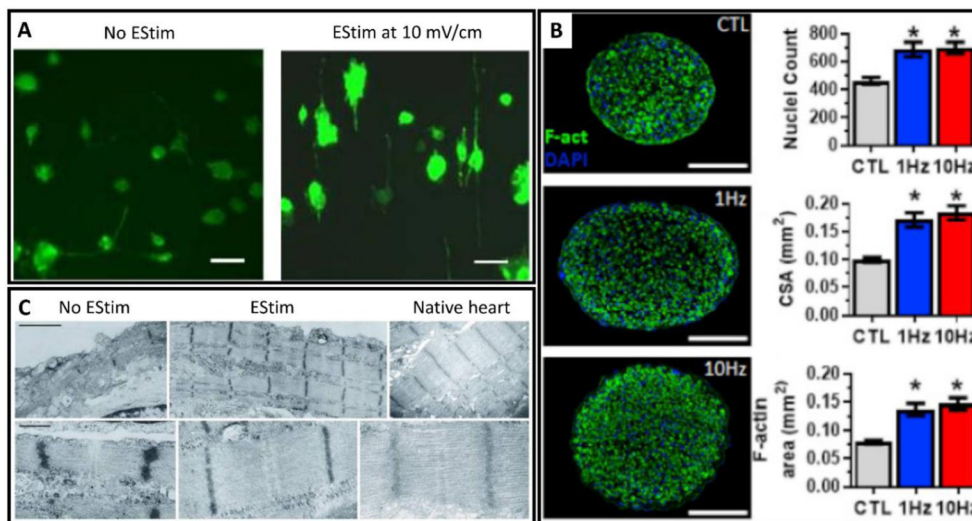


Fig. 4. EStim enhances tissue regeneration. (a) EStim increases the neurite length PC12 cells. Scale bars are 50 μm . Image reprinted from (109) with permission. Copyright 2009, Elsevier. (b) EStim (at 1 and 10 Hz) promotes growth of myobundles of human skeletal muscle. CTL is no-EStim control. CSA is myobundle cross-sectional area. F-act is filamentous actin. Scale bars are 200 μm . Image reprinted from (114) with permission. Copyright 2019, Elsevier. (c) EStim facilitates the assembly and ultrastructural development of cardiomyocytes, which is similar in many aspects to native myocardium. Bar is 2 μm in the first row and 1 μm in the second row. Image reprinted from (116) with permission. Copyright 2004, National Academy of Sciences

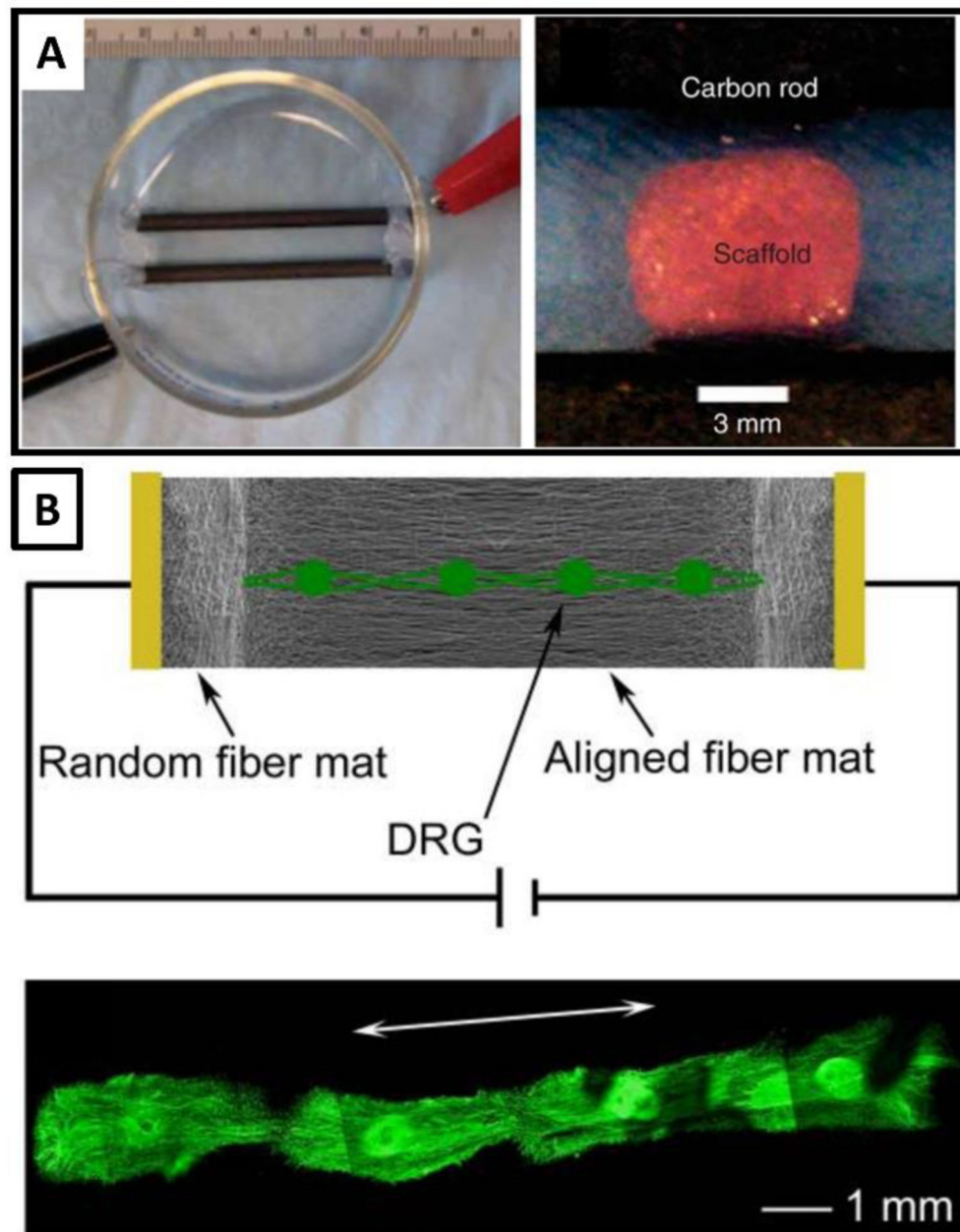


Fig. 5. Commonly used EStim setups for tissue engineering. (a) Carbon rod electrodes directly inserted in culture medium are used to deliver EStim. 3D scaffolds can be placed in between the electrodes. Image reprinted from (40) with permission. Copyright 2009, Springer Nature. (b) EStim can be applied through conductive nanofibrillar scaffold (PCL-PPy) to increase neurite length. Image reprinted from (107) with permission. Copyright 2009, John Wiley and Sons

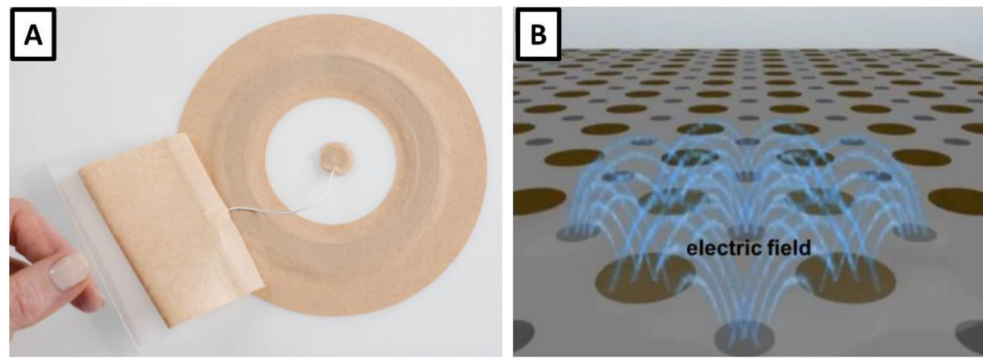


Fig. 6. Commercial EStim wound dressings. (a) POSiFECT®RD bioelectric dressing. Image reproduced from (154) with permission from Rafael V. Andino. Copyright 2006, Biofisica, Inc. (b) Procultura redox active bioelectric dressing. Image reproduced from (155) with permission under the terms of the Creative Commons Attribution License. Copyright 2014, Public Library of Science

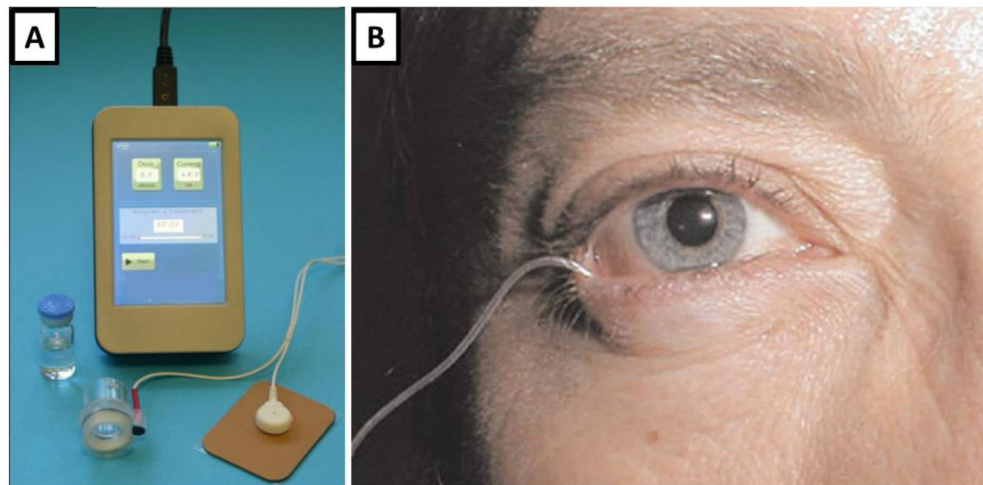


Fig. 7. Commercial iontophoretic ocular drug delivery devices. (a) The EyeGate II Delivery System. Image reproduced from (165) with permission. Copyright 2012 Elsevier. (b) OcuPhor iontophoretic device inserted in the eye. Image reproduced from (167) with permission under the terms of the Creative Commons Attribution License. Copyright 2011, Wolters Kluwer

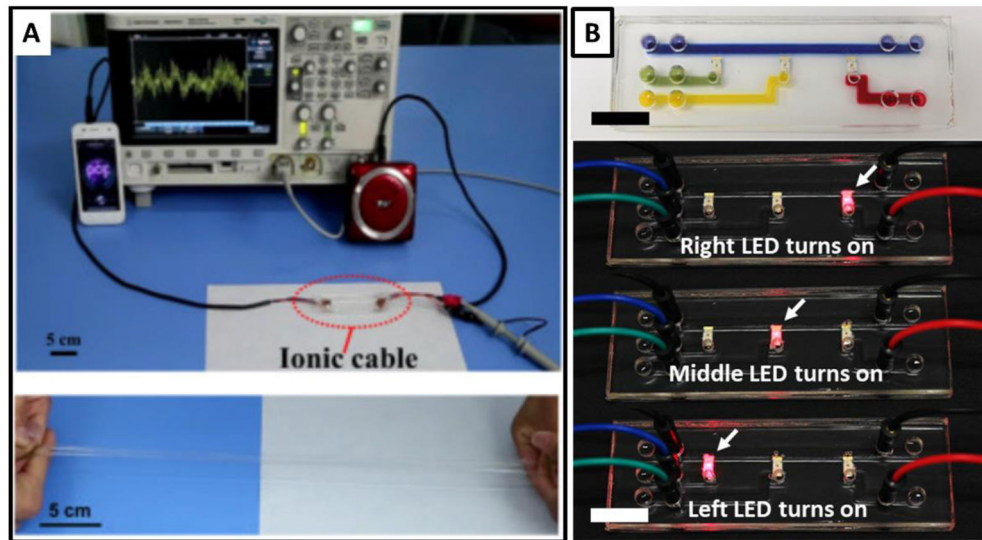


Fig. 8. Recent efforts to minimize device-tissue mismatch. (a) Ionic conductors are prepared with hydrogel materials infused with high concentration salt solutions. It can be used to prepare ionic cable to transmit music signal. Image reprinted from (179) with permission. Copyright 2015, Elsevier. (b) A hydrogel ionic circuit that can deliver ion current to activate LEDs. Scale bars are 1 cm. Image reprinted from (181) with permission. Copyright 2018, John Wiley and Sons

Table 1:

Common EStim modes and parameters used for each tissue type or application, and the typical outcomes of EStim.

Target tissue or application of EStim	Modes of EStim typically used	Common EStim parameters	Typical tissue/cell responses	Substrate for tissue engineering
Nerve (5)	DC, AC, PC, PEMF	Electrical voltage: 10 to 100 mV. Electrical current: up to 200 mA Frequency: DC or 1 to 500 Hz	Accelerated and directional neurite and axon growth, the differentiation of stem cell into the neural fate	Electrically conductive scaffolds are typically used for tissue engineering
Muscle (37, 38)	PC	Electrical current: up to 250mA. Frequency: 1 to 50 Hz. Pulse width: 10 μ s to 150 ms.	Proliferation and maturation of myoblast, expression of myosin heavy chain, alignment and elongation of cardiomyocytes, increased expression of connexin 43 and troponin-I, synchronous contractions of cardiomyocytes	Non-conductive natural or synthetic scaffolds are usually used for skeletal muscles. Conductive scaffolds have been used for cardiac tissue engineering
Bone (10)	DC, AC, PC, PEMF	Electrical current: 5 to 100 μ A (DC). Electrical field: 1 to 100 mV/cm (AC, PC and PEMF) Frequency: DC or 20 to 200 kHz (AC, PC) or 1 to 100 Hz (PEMF)	Increased calcium signaling and bone formation, upregulated bone growth factors, increased activity of osteoblast, increased production of VEGF	Both non-conductive and conductive scaffolds have been used for bone tissue engineering
Wound healing (13)	DC, AC, PC, PEMF	Electrical voltage: 5 to 300 V. Electrical current: 30 μ A to 20 mA. Frequency: DC or 0.8 to 600 Hz (AC, PC, PEMF)	Directional and accelerated migration of skin cells, increased proliferation of skin cells, bacteriostatic and bactericidal effects, increased blood perfusion	
Pain relief (39)	PC	Electrical current: up to 100 mA. Frequency: 50 to 200 Hz	Clinical trials showed inconsistent and inconclusive results regarding EStim efficacy on pain relief	
Drug delivery (1)	DC	Electrical current density: 0.8 to 25 mA/cm ² . Frequency: DC	Increased membrane permeability, increase mobility of drug molecules through electrophoresis and electroosmosis	